DESCRIPTION: State the application's broad, long-term objectives and specific aims, making reference to the health relatedness of the project. Describe concisely the research design and methods for achieving these goals. Avoid summaries of past accomplishments and the use of the first person. This abstract is meant to serve as a succinct and accurate description of the proposed work when separated from the application. If the application is funded, this description, as is, will become public information. Therefore, do not include proprietary/confidential information. **DO NOT EXCEED THE SPACE PROVIDED.**

The overarching goal of this proposed Imaging Core is to understand better the effects of prenatal alcohol exposure on the structure and function of the developing brain by facilitating the use of advanced brain image processing tools by CIFASD members. One of the key limitations in understanding the role of severe prenatal alcohol exposure on the developing brain has been the limited number of subjects studied by any single research group. It is our intent to use this opportunity to pool structural brain imaging data across multiple research sites by standardizing the imaging protocols used to acquire image data, and standardizing image analysis tools used to compare individuals with fetal alcohol spectrum disorders (FASD) to controls. We will use our expertise to provide members of the Consortium with access to relatively simple automated image analysis tools that they can use in their laboratories to assess the shape and size of the corpus callosum (CC) and other regularly shaped brain structures. More specialized tools will be developed to assess differences in brain morphology in cortical and subcortical structures and to combine functional and structural MRI data for within-project functional-structural MRI studies. Specifically, our efforts will be directed towards: 1) the standardization of image acquisition protocols and validation of methods for controlling scanner specific geometric distortion through the use of human and mechanical phantom studies; 2) the adaptation of automated image analysis tools for distribution to CIFASD members; 3) adaptation and creation of more sophisticated tools for assessment of brain shape and tissue distribution abnormalities in cortical and subcortical regions, and the refinement of tools designed to facilitate the combination of functional and structural brain imaging data; and 4) the assessment of relationships between brain image data, and data collected by the other CIFASD projects and cores. Consortium members are proposing to collect either functional or structural (or both) brain imaging data from over 470 children and adolescents with FASD and 310 control subjects. The strategies and methods developed within the Imaging Core will for the first time allow the direct comparison of data collected at various sites, dramatically increasing our power to potentially outline diagnostic criteria from brain imaging data, and ultimately to help develop intervention and treatment approaches for FASD.

PERFORMANCE SITE(S) *(organization, city, state)*

Laboratory of Neuro Imaging
Department of Neurology
UCLA School of Medicine
Los Angeles, CA 90095

KEY PERSONNEL. See instructions. *Use continuation pages as needed* to provide the required information in the format shown below. Start with Principal Investigator. List all other key personnel in alphabetical order, last name first.

Name	Organization	Role on Project
Sowell, Elizabeth R.	UCLA Department of Neurology	PI
Shattuck, David W.	UCLA Department of Neurology	Investigator
Toga, Arthur W.	UCLA Department of Neurology	Co-PI

Disclosure Permission Statement. Applicable to SBIR/STTR Only. See instructions. ☐ **Yes** ☐ **No**

A. Specific Aims

The specific aims of the Imaging Core are to develop new brain image analysis tools, modify existing tools, and disseminate to members of the Consortium these tools for quantifying brain abnormalities in individuals with "fetal alcohol spectrum disorder" (FASD) studied with magnetic resonance imaging. One of the key limitations in understanding the role of severe prenatal alcohol exposure on the developing brain has been the limited number of subjects studied by any single research group. It is our intent to use this opportunity to pool structural brain imaging data across multiple research sites by standardizing the imaging protocols used to acquire image data, and standardizing image analysis tools used to compare individuals with FASD to controls. State-of-the-art brain image analysis methodology which allows quantitative assessment of brain dysmorphology in FASD is quickly advancing, highly technical and requires considerable computing resources and extensive training. The Brain Imaging Core will bring all these aspects of their resources and experience to all Consortium members, significantly enhancing each Consortium investigator's ability to exploit their expensive imaging data. We will use our expertise to provide members of the Consortium with access to user-friendly automated image analysis tools that they can use to assess the shape and size of the corpus callosum (CC) and other regularly shaped brain structures. More specialized tools will be developed to assess differences in brain morphology in cortical and subcortical structures and to combine functional and structural MRI data for within-project functional-structural MRI studies. Further, we will provide to Consortium members with access to all hardware and software available at the Laboratory of Neruo Imaging (LONI) which is one of the most sophisticated established laboratories in the world dedicated to brain image analysis. The Imaging Core will be integrated with the other scientific Consortium Cores, and will assess the following 4 specific aims.

1. Image Acquisition Calibration: We will scan a human volunteer and a mechanical phantom on all magnets that will be used to collect structural MRI data in order to establish the protocols and parameters for scanner calibration to correct scanner-specific geometric distortion. In order to calibrate data collected from each scanner, we will calculate the deviation in spatial registration between phantom (human and mechanical) images collected at each site, and apply spatial correction algorithms to ensure that they are anatomically (and geometrically) matched. We will work with other Consortium members to help them best perfect their image acquisition protocol that may vary somewhat by magnet manufacturer.

2. Automated Tools for Distribution: We will adapt automated image analysis tools for dissemination to the various sites collecting structural brain imaging data to assess CC shape and other brain structural information. All software adapted and created for the purposes of this Consortium will be platform independent, and user-friendly. The Imaging Core will provide training via web-based, in-person and email supported mechanisms on the use of the tools, and conduct shape analyses on the CC contours provided by the various imaging groups within the Consortium.

3. Adapted Tools for Detailed Surface Analyses: We will create and adapt more sophisticated tools to be used within LONI applied to structural imaging data collected at various sites. Further, we will adapt tools for combining structural and functional MRI data for those sites collecting these types of imaging data. These tools will be used to assess brain dysmorphology in cortical and subcortical brain regions of interest, and to account for structural variability when assessing functional signal using MR spectroscopy or functional MRI. In this instance, it is envisioned that imaging data from all interested participating sites would be transferred to LONI where dedicated staff would conduct image and statistical analyses under the supervision of the Imaging Core PIs, and in collaboration with the consortium members collecting the imaging data.

4. Correlation with Other Core Data: We will assess for relationships between the data collected and analyzed within the Imaging Core, and data collected by the other projects and cores in this Consortium such as the Dysmorphology Core, the Neurobehavioral Core, and the Facial Imaging Core. We currently have statistical tools which allow us to map linkages (via correlation, multiple regression, multivariate, non-linear regression) between brain morphology (i.e., gray matter density, local brain size) at every brain surface point and any measure collected by the various other projects and cores.

B. Background and Significance

The need for advanced brain image analysis technology is critical for understanding FASD about whose brain maturation we know so little. The recent advancement in *in vivo* brain imaging technology has largely focused on adult populations and the validity of its application to developmental populations is less clear. This is because, as discussed in the following paragraphs, the size, shape, tissue distribution, and functional capacity of the brain are continually evolving at different rates and in different brain regions and these normative maturational processes are disrupted by prenatal alcohol exposure. In the past few years, we have created advanced image analysis tools at LONI to measure structural aspects of these 4-dimensional changes (i.e., orthogonal x, y, and z coordinates with time being the 4th dimension) in the developing human brain. Drs. Elizabeth Sowell and Arthur Toga, the Co-Principal Investigators on this proposed project, have collaboratively integrated the surface-based structural image analysis algorithms originally developed at LONI into their studies of FASD. This project is innovative because the investigators will use these advanced image analysis tools in the larger study of FASD individuals afforded by the collaborative nature of this Consortium. We will further develop these algorithms for application to high resolution structural magnetic resonance image data collected by the various Consortium participants, and we will also adapt tools for assessment of functional imaging data sets (i.e., fMRI, MR spectroscopy).

How Is This Proposal Responsive to the Request for Applications? This Imaging Core Proposal addresses issues that are expressly implicated in the request for proposals (RFA AA-03-002). Specifically, the RFA states that:

> "This core may provide imaging services to the components. Such a core could focus on multiple imaging technologies. Technology research and development of innovative new imaging technologies appropriate for FASD research in humans (and/or animal models), as well as refinement and development of technologies already established may also be an additional focus of this core."

In the following sections, we will illustrate our expertise and leadership in the field of brain image analysis, and ultimately our ability to address the specific requirements of the entire Consortium project and this RFA. Further, we will show how we have begun to apply new image analysis technologies in the study of FASD, and how we will advance the field of FASD research with new approaches to brain image analysis using the large sample of subjects collected by CIFASD members. The Brain Imaging Core will be an integral part of the entire CIFASD proposed as we will allow assessment of linkages between brain anatomy, and all other data types collected by Consortium members. We will show depictions of these relationships by creating brain maps that explicitly define regions where brain anatomy is correlated with neurobehavioral or facial morphological variables. Thus, the activities of all other projects and cores will be enhanced by the efforts of the Imaging Core. In turn, the Imaging Core will benefit from the other cores and projects by an enhanced understanding of correlates of brain dysmorphology resulting from prenatal alcohol exposure.

How Are the Principal Investigators Qualified to Conduct the Proposed Studies? As outlined in the preliminary studies section below, extensive investigations into brain structural abnormalities in FAS have been conducted by the principal investigators resulting in 5 peer reviewed publications thus far. Dr. Elizabeth Sowell has been integral in helping design and implement the structural image analysis tools in collaboration with Dr. Arthur Toga, the Co Principal Investigator on this Imaging Core. Dr. Sowell has a long history of structural MRI investigations in developmental populations, and her training in clinical neuropsychology has enhanced her ability to design and implement functional paradigms to tap brain regions of interest in the FAS population. Dr. Arthur Toga has extensive experience in the processing of data from multiple sources and the management of information from a wide range of image acquisition devises (e.g., Computational Anatomy and Multidimensional Modeling, NCRR 2P41RR013642-05; International Consortium for Brain Mapping, ICBM, P01 MH52176; Biomedical Informatics Research Network, Brain Morphology BIRN, 02076682 (M01 RR00827)). Thus, the proposed Principal Investigators are well poised and highly qualified to conduct the proposed studies. It is also important to note that the Principle Investigators of the Imaging Core have a long-standing collaborative relationship with Dr. Ed Riley, the overseer of the CIFASD proposal and proposed PI of the

administrative core of this Consortium. This speaks well of our potential for continued fruitful collaboration if the CIFASD is funded.

Overview of Fetal Alcohol Syndrome: Fetal Alcohol Syndrome (FAS) is a permanent birth defect caused by maternal consumption of alcohol during pregnancy, and it is a leading cause of preventable developmental disabilities. Despite the common lay perception that the teratogenic effects of alcohol on the fetus are static, our recent studies have shown that brain growth continues to be adversely affected during childhood and adolescence, long after the prenatal insult of alcohol exposure to the developing brain. Briefly, FAS describes a constellation of symptoms often found in infants born to alcohol abusing mothers (Jones and Smith, 1973). These symptoms include prenatal growth deficiency, developmental delay, craniofacial anomalies (i.e., microcephaly, epicanthal folds, short palpebral fissures), and limb defects. Roughly 10 to 40% of children born to alcohol abusing mothers meet criteria for the diagnosis (Jones and Smith, 1973; Abel and Sokol, 1987). Brain abnormalities, most commonly microcephaly and neuronal migration anomalies, have been documented in *post mortem* studies (Jones and Smith, 1973; Roebuck et al., 1998). Mental retardation is common among FAS individuals (Abel and Sokol, 1987) and subtler neuropsychological abnormalities have also been reported (Mattson and Riley, 1998). Additionally, behavioral and psychosocial problems are frequently observed in these subjects (Roebuck et al., 1999). Our structural MRI studies have already shown abnormalities in the tissue distribution and the shape of the brain in children with FAS and even in children with severe prenatal alcohol exposure but without facial dysmorphology (referred to as PEA) required for the FAS diagnosis. Functional studies are also critical to our understanding of the impact of brain dysmorphology on brain function, but no functional MRI studies have yet been published in FASD. From the structural abnormalities in alcohol-exposed children, inferences can be made about the functional impact, but only with detailed functional imaging studies, such as those proposed by various projects in this Consortium, can these inferences be confirmed.

Structural Imaging Studies in FAS: *In vivo* quantitative magnetic resonance imaging (MRI) studies have confirmed brain morphologic abnormalities in children prenatally exposed to alcohol, and have allowed a more detailed account of some of the subtler structural dysmorphology previously observed in these subjects in post mortem studies. Recently, we have applied whole-brain MR image analysis techniques to a group of children, adolescents and young adults with prenatal alcohol exposure. The first of these studies (Archibald et al., 2001) utilized volumetric methods, and showed that within the cortex, only the parietal lobes were significantly reduced in volume above and beyond the generalized microcephaly observed in these subjects. It also showed that white matter hypoplasia was more significant than gray matter hypoplasia and relative sparing of hippocampal volume was noted. Other research groups have also used quantitative methods to document generalized microcephaly (Swayze et al., 1997). In another study by our group of the same alcohol exposed (ALC) subjects, voxel-based morphological analyses were conducted where brain tissue abnormalities in the whole brain were analyzed at once on a voxel-by-voxel basis. Results from this study (Sowell et al., 2001c) complemented findings from the volumetric studies revealing abnormalities most prominently in the perisylvian cortices of the temporal and parietal lobes where the ALC subjects tended to have increased gray matter density and decreased white matter density. These findings are also consistent with what would be expected given our studies of corpus callosum morphology in ALC subjects which show that the regions of the corpus callosum that connect perisylvian cortices between the two hemispheres are the most severely affected (Sowell et al., 2001b). Quantitative methods were also used by another research group to document callosal shape abnormalities in FAS (Bookstein et al., 2001).

While the volumetric and voxel-based image analyses described above tended to localize cortical tissue abnormalities to parietal lobe regions, we became interested in abnormalities on the overlying cortical surface of the brain. Thus, in another study (Sowell et al., 2002a) we analyzed brain surface shape abnormalities in the same group of children, adolescents and young adults with prenatal alcohol exposure and assessed relationships between cortical gray matter density on the brain surface and brain shape. We carefully matched brain surface anatomy across individuals by defining cortical sulcal landmarks identified on the brain surface of every individual, thereby ensuring accurate localization of group differences relative to sulcal landmarks. Understanding spatial and temporal relationships between brain shape on the one hand, and tissue density

changes on the other hand, could help shed light on the biological processes contributing most to the brain dysmorphology in the individuals observed in earlier structural MRI studies. Additionally, understanding the relationships between regional and temporal patterns of abnormal brain shape and cortical tissue density abnormalities could provide further insight into patterns of cognitive and behavioral deficits characteristic of FAS. Analyzing brain shape in these surface-based analyses allowed us to assess regional abnormalities in brain volume, independent of the tissues that comprise the brain in any given region, and without the limitations of volumetric studies where regional boundaries must be identified. We predicted that we would see shape abnormalities in the perisylvian and inferior parietal regions, the same regions where we observed increased cortical gray matter density in these subjects in the earlier reports (Sowell et al., 2001c). While we did not see evidence for frontal lobe abnormalities in the volumetric (Archibald et al., 2001) or voxel-based (Sowell et al., 2001c) analyses of these subjects, we predicted that we would observe frontal lobe anomalies that might not be reflected in the volumes or tissue density of these regions. This hypothesis was based on the cognitive and behavioral literature which suggests that children with prenatal alcohol exposure have difficulties with response inhibition, behavioral control, and executive functions (Olson et al., 1998; Mattson et al., 1999), all known to be related to frontal lobe functioning. Results showed significant brain size and shape abnormalities in the alcohol-exposed subjects in inferior parietal/perisylvian regions bilaterally where their brains appeared to be narrower than the controls' in the same general location where they also had increased gray matter density. Highly significant decreased brain surface extent or reduced brain growth was also observed in the ventral aspects of the frontal lobes most prominent in the left hemisphere. The results imply that brain growth continues to be adversely affected long after the prenatal insult of alcohol exposure to the developing brain and the brain regions most implicated, frontal and inferior parietal/perisylvian, may be consistent with neurocognitive deficits characteristic of individuals prenatally exposed to alcohol.

Neuropsychological Findings in FAS: Also associated with prenatal alcohol exposure are ongoing cognitive and behavioral impairments (Mattson et al., 1999); (Olson et al., 1998; Mattson and Riley, 1999). Results from neuropsychological studies have not thus far isolated a stable profile of strengths and weaknesses. Among the more robust impairments observed in these patients, however, are in areas of attention (Streissguth et al., 1995); (Coles et al., 1997), verbal learning (Mattson et al., 1996), executive functions (Mattson et al., 1999) and perhaps visuomotor functioning (Mattson and Riley, 1998; Olson et al., 1998).

Parietal and frontal lobe functioning in FAS patients are of particular interest given the brain shape and tissue density abnormalities found in these regions in the structural imaging studies (Sowell et al., 2002a). Uecker and Nadel reported rather profound constructional apraxia in a group of FAS children and adolescents (Uecker and Nadel, 1996). These children had difficulty translating their perception of a clock to a visual representation, and had difficulty copying geometric designs, both of which are frequently associated with parietal lobe damage (Lezak, 1995). Another group also showed problems with visuomotor integration in children with FAS (Janzen et al., 1995) further confirming their difficulty with functions typically subserved by the parietal lobes. Mattson and colleagues detailed executive/frontal lobe functioning in a group of children and adolescents with severe prenatal alcohol exposure (Mattson et al., 1999). Specifically, they found that these children had difficulty with switching between cognitive sets, response inhibition, analytical thinking and planning, all of which are associated with frontal lobe deficits (Lezak, 1995).

Functional Imaging Studies in FAS: To date, no functional activation studies have been reported in the human prenatal alcohol exposure literature but a few reports of resting brain metabolic activity have been described. Riikonen and colleagues (Riikonen et al., 1999) reported findings of brain perfusion abnormalities in FAS children using single positron emission tomography (SPECT). The patients lacked the "normal left-right dominance" due to hypoperfusion of the left parieto-occipital region and also of the right frontal region. Another research group found decreases in cerebral metabolic rates in bilateral thalamic and basal ganglia regions using positron emission tomography (PET) (Clark et al., 2000). Clearly, results from theses studies suggest that in addition to the structural abnormalities, brain function is altered as a result of severe prenatal alcohol exposure. However, it is not yet clear how brain structure, brain metabolic activity, and brain activation are related in this population.

What Will Be Gained from the Imaging Core: While much has been learned about the effects of prenatal alcohol exposure on the brain from these studies, most of the literature is based on small samples (n < 25). The reproducibility of the extant findings have not been assessed in independent samples, and the image analysis methods used by the various research groups have not yielded comparable results. It is the aim of the Imaging Core to begin to standardize image analysis procedures and acquisition protocols, to assess the comparability of FASD children across research sites. We will have a unique opportunity in this forum to assess brain morphology in as many as 470 children with FASD.

C. Preliminary Studies

This Core will help homogenize the acquisition of image data from multiple sites and help integrate the disparate types of data being collected in the project. The image data will be organized in a way that provides indexes between the clinical and other data being collected. Visualizations that depict multiple and varied observations from the other cores and projects will describe the statistical relationships in a compelling and intuitive way. Some of our preliminary work utilizing the image analysis tools currently available at LONI for integration of brain image and neurobehavioral data are described below. As outlined even further in the Research Design section, improvement of the current tools, and creation of new tools will be an express aim of the Imaging Core allowing more in-depth integration of disparate data types.

In the last 3 years, we have conducted detailed analyses of brain structural dysmorphology in a group of 21 children and adolescents with severe prenatal alcohol exposure as compared to 21 normally developing children and adolescents. Results from these studies have prompted us to plan explorations of brain functional abnormalities in conjunction with the structural imaging studies and we have obtained independent funding for data collection (NIDA 1R21DA015878-01, PI E. Sowell). Combining the functional and structural data using continuum mechanical warping algorithms have been challenging, but we have conducted some promising pilot studies that serve as a bounding-board for the procedures we will apply to data collected by Consortium members. All of the data analysis strategies described in the Preliminary Studies can be applied to image data collected from various Consortium sites. Their application to data sets from various regions, and the combining of these data will provide immense new power to validate previous findings, and elucidate new knowledge about the effects of prenatal alcohol exposure on the developing brain. Following is a list of preliminary studies to be described:

1) Brain Shape and Tissue Density Abnormalities in Prenatal Alcohol Exposure Assessed with Surface-Based algorithms (Specific Aims 2 and 3)
2) Functional Imaging Studies with Advanced Warping Strategies (Specific Aim 3)
3) Brain Shape Correlated with Other Types of Data (Specific Aim 4)

1) Brain Shape and Tissue Density Abnormalities in Prenatal Alcohol Exposure Assessed with Surface-Based algorithms (Specific Aims 2 and 3):

Using the surface-based continuum mechanical warping algorithms developed at LONI, we have assessed shape changes in the morphology of the corpus callosum (CC) (Sowell et al., 2001b), tissue density abnormalities (Sowell et al., 2002a), brain shape differences (Sowell et al., 2002a), and brain surface and gray matter density asymmetry (Sowell et al., 2002c) in the alcohol-exposed subjects. All of these studies were conducted with the same subject sample (described below) recruited and imaged by Edward Riley, the PI of the Administrative Core of this Consortium, and his colleagues in San Diego.

Subjects: The patient group consisted of 20 children, adolescents, and young adults between the ages of 8 and 22 years (mean age 13 years; 10 female, 2 left handed) who were prenatally exposed to alcohol (ALC). All of the children and young adults had histories of behavioral problems, cognitive impairment, and heavy prenatal alcohol exposure. Thirteen of them had the characteristic facial appearance (Jones et al., 1973) that allowed for a diagnosis of fetal alcohol syndrome (FAS; mean age 12.8 years, 7 female; 1 left handed). Seven

other subjects did not have the facial features to warrant a diagnosis of FAS, and are instead referred to as subjects with prenatal alcohol exposure (PEA; mean age 13 years, 3 female, 1 left handed).

In addition to the group of ALC subjects, 21 normal children, adolescents and young adults between 8 and 25 years were studied as a comparison group (mean age 13.5, 12 female; all right handed).

Imaging Protocol: MR was performed with a 1.5 Tesla magnet (Signa: General Electric, Milwaukee). A gradient-echo (SPGR) T_1-weighted series was collected for each subject with TR=24 ms, TE=5 ms, NEX=2, flip angle=45 degrees, field of view of 24 cm, section thickness of 1.2 mm, no gaps, with an imaging time of 19 minutes.

Corpus Callosum Morphology: The corpus callosum was manually traced for each subject on the midsagittal slice of the spatially normalized brain volumes and the contours were averaged to quantify within and between-group variations in callosal shape. Callosal surfaces/edges were also divided into inferior and superior sections with 5 equal length pieces across the horizontal callosal axis for assessment of regional variability in displacement and regional callosal area.

Striking differences between ALC and control subjects were observed in the group average and CC displacement maps (see Figure 1). Note the inferior and anterior displacement of the CC in posterior splenial and isthmus regions, with the relative sparing of more anterior genu and mid-body regions. These dramatic effects were observed whether analyzed in native space prior to scaling, or in standard space. The significant group effects in repeated measures analyses of superior displacement and anterior displacement on the top surface of the CC indicated that it was displaced overall in the ALC subjects relative to the controls. Group by region interactions were at trend level significance indicating that not all regions were displaced uniformly. Follow-up tests provided quantitative evidence that the posterior regions were more anteriorly and inferiorly displaced in the ALC subjects than were the more anterior regions.

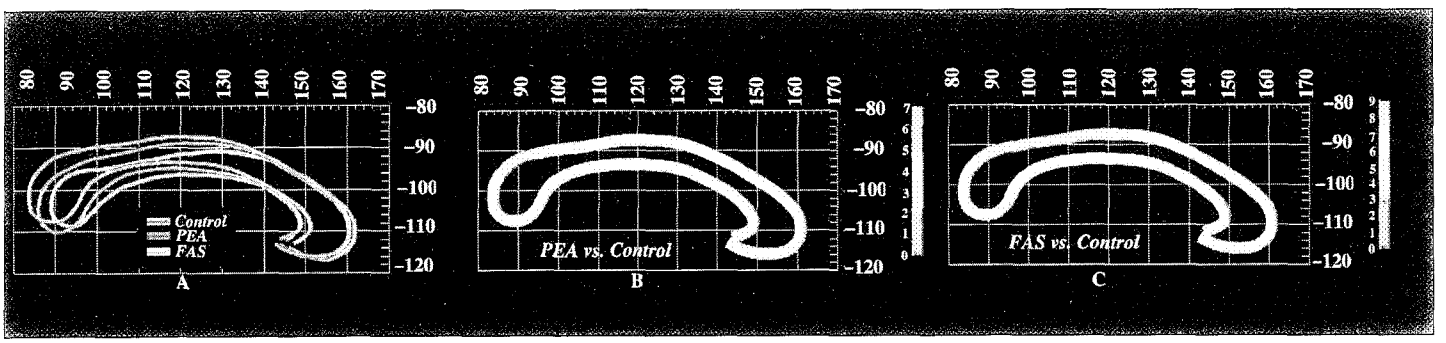

Figure1: **(A)** Average callosal lines in ICBM-305 Standard space showing the distinctions between FAS, alcohol exposed non-FAS children (PEA) and Control subjects. Note the placement of the CC in PEA subjects somewhere between that of the control and FAS subjects, but with a similar pattern of displacement. **(B)** Map showning average displacement vectors in millimeters between the PEA and control subjects, and **(C)** between the FAS and control subjects. Again, the pattern of displacement is the same in the PEA subjects, but the displacement is somewhat less severe than that observed for the FAS subjects.

Findings from this study (Sowell et al., 2001b) are particularly relevant to the proposed studies because neurocognitive measures were found to be significantly correlated with callosal dysmorphology. Specifically, the amount of CC displacement was correlated with impairment in verbal learning ability. Additionally, CC displacement (i.e., a measure of shape) was found to be better predictor of verbal learning than regional CC area (i.e., a gross measure of size), and these relationships were not solely mediated by overall impaired verbal intellectual functioning. These were the first findings to our knowledge of correlations between quantitative measures of brain dysmorphology in FASD, and provide support for our intention to assess correlations between brain image data, and neurobehavioral data collected for the same individuals by the various Consortium sites.

This study relates directly to Specific Aim 2 in the Imaging Core where we propose to have Consortium members utilize automated image analysis tools developed at LONI to define the CC and other regularly shaped brain structures. Improved reliability, and the potential for processing large numbers subject's imaging data are an advantage of the proposed automated methods.

Tissue Density and Brain Shape Abnormalities: MR images from each individual were processed with a series of manual and automated procedures that included the following steps: (i) each image volume was roughly resliced into a standard orientation by trained operators who "tagged" 10 standardized anatomical landmarks in each subject's image data set that corresponded to the same 10 anatomical landmarks defined on the ICBM-305 average brain (Mazziotta et al., 1995). Next, brain image volumes were more carefully spatially registered to *each other* by defining 80 standardized, manually defined anatomical landmarks (40 in each hemisphere, the 1st and last points on each of 20 sulcal lines drawn in each hemisphere shown in Figure 2) in every individual, and using a least-squares rigid-body transformation to match each individual to the average of all individuals in the data set; (ii) classification of brain images into gray matter, white matter, and cerebrospinal fluid (CSF); (iii) removal of non-brain tissue (i.e., scalp, orbits) and cerebellum from the transformed images; (iv) automated extraction of the cortical surface for each individual shown in Figure 2 (MacDonald et al., 1994); (v) tracing of 23 sulcal and gyral landmarks in each hemisphere on the cortical surface rendering of each individual (Sowell et al., 2002b) shown in Figure 2; (vi) estimating gray matter density or local gray matter proportion (measured as the amount of segmented gray matter within a sphere attached to each anatomically matched surface point) over the entire cortical surface of each individual's brain (Sowell et al., 2001a; Sowell et al., 2002b); and (vii) estimating relative local brain growth measured at each cortical surface point as shown in Figure 4 (i.e., the radial expansion or distance from the center (DFC) of the brain near the anterior commisure to each cortical surface point) (Sowell et al., 2001a).

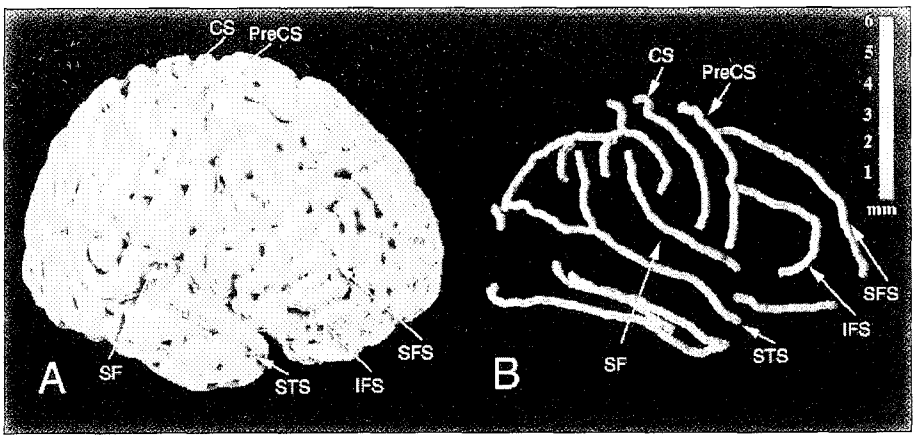

Figure 2: A. Sample surface rendering with sulcal lines shown in pink (Sylvian fissure, and central, pre-central, post-central, superior temporal sulcus (STS) main body, STS ascending branch, STS posterior branch, primary intermediate sulcus, secondary intermediate sulcus, inferior temporal, superior frontal, inferior frontal, intraparietal, transverse occipital, olfactory, occipito-temporal, and collateral sulci) B. Interrater reliability map representing the average difference (in millimeters of displacement) of 6 subjects' sulci drawn by 2 independent raters.

After the basic preprocessing steps were conducted for each individual, statistical maps of differences between groups were created for gray matter density and DFC. In these analyses, the correlation (Pearson's r) between group membership and (1) gray matter density or (2) DFC at each brain surface point was calculated. Permutation tests were conducted to assess the significance of the statistical maps (gray matter and DFC) and to correct for multiple comparisons. Anatomical regions of interest (ROI; frontal, parietal, temporal and occipital lobes) were used in the permutation analyses to test our *a priori* hypotheses for DFC that we would see abnormalities in perisylvian and frontal regions. The number of surface points within each ROI that was significant at a threshold of $P = 0.001$ (for the DFC analyses) was compared to the number of significant surface points within the ROI that occurred by chance when subjects were randomly assigned to groups in 10,000 new analyses.

A statistical map of differences in gray matter density between the ALC and control subjects is shown in Figure 3. Note the large regions in the inferior parietal and perisylvian cortex bilaterally (more prominently in the left hemisphere) where the gray matter density is increased in the ALC subjects relative to control subjects. This result was expected given our earlier findings where voxel-based morphometry was used (Sowell et al., 2001c). However, when surface-based warping algorithms were used, gray matter density at homologous

anatomical surface points was insured given that each subject's anatomy was matched on surface sulci rather than relying on automated methods for anatomical matching used in the voxel-based morphometry report. The ALC subjects have an estimated 15% more segmented gray matter in the regions where group differences are significant. Note that the highly significant gray matter density increases measured here are also likely reflective of reductions in white matter in the perisylvian regions, given that less gray matter tissue at each surface point means that more white matter or CSF is present. Permutation analyses within lobar ROIs confirmed the significance of the tissue abnormality spanning across the perisylvian cortices of the parietal lobes bilaterally ($p < 0.001$ L and R hems) and the temporal lobes, particularly in the left hemisphere (L hem $p < 0.001$, R hem $p < 0.01$).

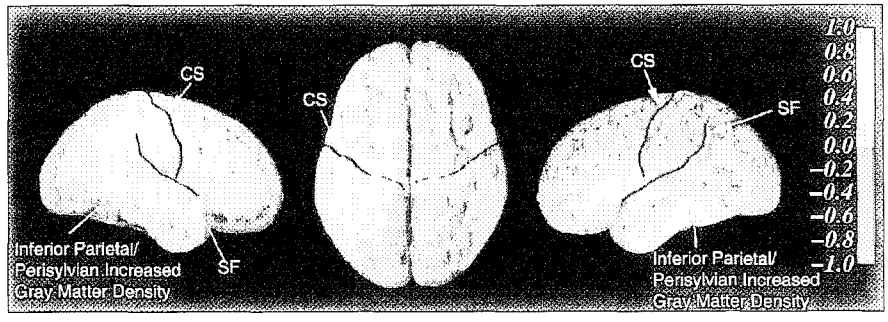

Figure 3: Gray matter density group-difference statistical maps showing gray matter density increase (and white matter density decrease) in the ALC subjects relative to controls (in non-scaled space). Shades of green to yellow represent positive Pearson's correlation coefficients (increased gray matter density in ALC subjects) and shades of purple and pink represent negative Pearson's correlation coefficients (decreased gray matter density in ALC subjects) according to the color bar on the right (range of Pearson correlation coefficients from –1 to +1). Regions shown in red correspond to correlation coefficients that show significant increase in gray matter in the ALC subjects relative to controls at a threshold of $P = 0.01$. Regions shown in white correspond to correlation coefficients that show significant decrease in gray matter in the ALC subjects relative to controls at a threshold of $P = 0.01$. The Sylvian fissure (SF) and central sulcus (CS) are highlighted for anatomical reference.

Brain Shape group effects (ALC minus controls) are shown in Figure 4 where the difference in brain surface extent or local brain growth (i.e., DFC) in millimeters between the ALC subjects and controls is illustrated according to the color scale. Note first that the average brain surface extent is smaller in the ALC subjects in most locations as would be expected given their microcephaly. Prominent regional patterns emerge when size and shape differences are considered on a point-by-point basis over the entire brain surface. DFC in inferior parietal/perisylvian regions bilaterally is dramatically reduced by approximately 4 to 6 mm in the ALC subjects. The orbital frontal cortex, particularly in the left hemisphere is also considerably reduced. These are regions where the cortical surface is closer to the center of the brain in the ALC subjects, perhaps where there has been less local brain growth. The dorsal frontal and occipital cortex appear least affected with only approximately 0 to 1 mm difference between groups. A statistical map of DFC differences shows that the relatively large group differences in bilateral inferior parietal/perisylvian cortices and in the left orbitofrontal cortex are statistically significant (Figure 4). ROI permutation tests confirm the significance of DFC decreases (while correcting for multiple comparisons) in the ALC group in parietal, temporal, and frontal lobes.

Results from these studies reveal significant brain shape abnormalities in individuals prenatally exposed to alcohol, generally supporting our *a priori* hypotheses. Specifically, robust abnormalities are observed in the lateral perisylvian and parietal regions where the ALC subjects' brains appear to be too narrow. We also show new findings of decreased brain surface extent in the orbital frontal cortex. Findings of tissue density abnormalities localized primarily to large regions of inferior parietal and superior temporal cortex bilaterally replicate our results from an earlier report (Sowell et al., 2001c) where automated image registration was used. However, by using these novel surface-based methods, we have now been able to localize relatively small regions of gray matter volume increase within the temporal lobes surrounded by much larger regions of gray matter volume reduction. These effects could not be detected in more traditional volumetric studies where the temporal lobes were measured as a whole (Archibald et al., 2001). Finally, here we reveal a spatial distribution of brain surface extent reduction (i.e., decreased DFC) in the ALC subjects that is spatially quite consistent with, but inversely related to the pattern of gray matter density increase. That is, we tend to see regions of

increased gray matter density in ALC subjects spatially overlapping with regions of less local growth or lateral extension of the brain.

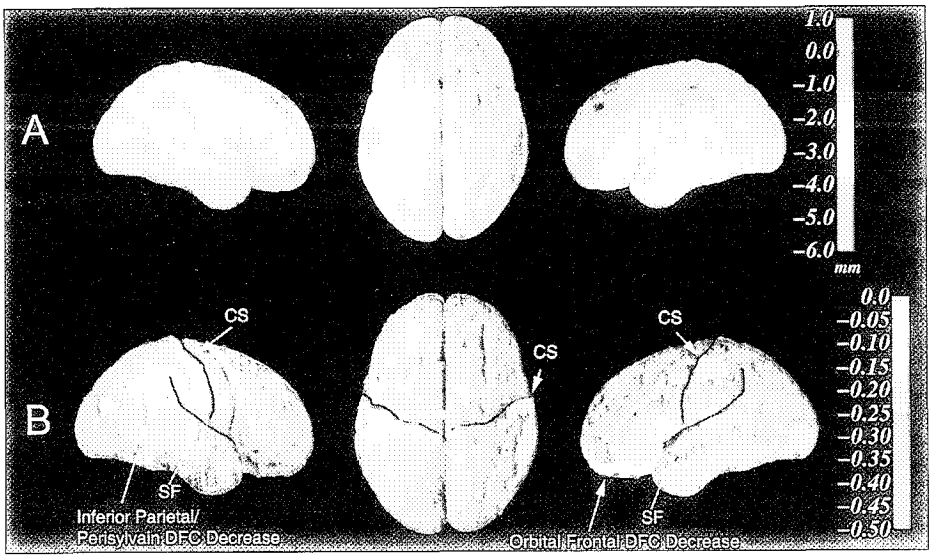

Figure 4: In the top row (A) are DFC group-difference maps showing differences in DFC (in mm) between the ALC and control subjects according to the color bar on the right. Notice the negative effects in nearly all regions meaning DFC is greater in the controls than the ALC subjects, with regional patterns of DFC reduction up to 6 mm. (B) DFC group-difference statistical maps showing differences in DFC between the ALC and control subjects in resliced (non-scaled) space according to the color bar on the right. As shown, most regions have negative Pearson's correlation coefficients (decreased DFC in ALC subjects relative to controls). Regions overlaid in white correspond to correlation coefficients that show significant decrease in DFC in ALC subjects at a threshold of $P = 0.001$.

Brain Surface and Gray Matter Asymmetry: Differences in brain surface location between the 2 hemispheres were computed for each subject by computing a flow of each subjects left hemisphere onto a flipped version of their right hemisphere while matching sulcal and gyral patterns. In this way, we could assess the distance in millimeters between analogous anatomical points in the left and the flipped, "sulcally matched" right hemispheres. We then used these flipped sulcally matched brain surface representations to assess ratios of gray matter density at analogous surface points (mapped back to the appropriate locations in the gray matter maps for each individual) in the left and right hemispheres. Note that in all of these analyses, 2 independently selected control groups were used to assess the validity of the asymmetry findings in normal controls before investigating group differences between ALC and control subjects. The control subjects scanned in San Diego (referred to as SDC) were used in all *group* comparison statistical analyses. A group of 62 normal control subjects between 7 and 25-years (mean age 14.9; 26 female; 60 right handed) were recruited and studied at the Yale Child Study Center (referred to as YC) as controls for individuals with tic disorders (described in (Peterson et al., 2001)). Hemispheric differences for gray matter density and surface location were also assessed in this group of control subjects.

After the basic preprocessing steps were conducted for each individual, statistical maps were created of *hemispheric* differences in surface point location between the left and "sulcally matched" right hemisphere within each group (i.e., ALC, SDC, YC). In these analyses, the correlation (Pearson's r) between hemisphere (coded as 0 for left hemisphere and 1 for right hemisphere) and the y-coordinate location was assessed at each brain surface point. The difference in y-coordinate location between hemispheres at any brain surface point had to reach a threshold of $p = 0.01$ to be considered significant. Analyses were also conducted to assess for *group* differences in the distance between y-coordinates in the left and right hemispheres at each brain surface point. We used similar methods to assess for differences in gray matter density between the left and right hemispheres within each group. In these analyses, the correlation (Pearson's r) between hemisphere (dummy coded as 0 for left hemisphere and 1 for right hemisphere) and gray matter density was assessed at each brain surface point. The difference in gray matter density between hemispheres at any brain surface point had to reach a threshold of $p = 0.05$ to be considered significant. Finally, we assessed *group* differences in the ratio of left to right gray matter at each brain surface point. Anatomical regions of interest (ROI) from a probabilistic atlas (Evans et al., 1996) were used in the permutation analyses to assess regional specificity of the brain surface and gray matter density asymmetry measures. The number of surface points within each ROI that were significant at a threshold of $P = 0.01$ were compared to the number of significant surface points within the ROI that occurred by chance when subjects (or hemispheres) were randomly assigned to groups (or

sides) in 10,000 new analyses. The permutations allowed us to determine the null distribution to assess the overall statistical significance of our results within the 4 ROIs.

Quantitative maps of brain surface asymmetry (Figure 5) reveal prominent perisylvian hemispheric differences in which the superior temporal and inferior parietal cortices are shifted backward in the left hemisphere in both normal and alcohol exposed subjects. Cortical surface gray matter asymmetry (Figure 6) is most prominent in the posterior inferior temporal lobes (right greater than left), and this effect does not differ between groups of normally developing children, adolescents, or young adults. Alcohol exposed individuals show a significant reduction in this asymmetry, whether studied with surface-based or more traditional volumetric region of interest analyses. This region of cortex (see Figure 7), near the junction of Brodmann's areas 21, 22, and 37, primarily subserves language functions that are known to be impaired on average in the alcohol-exposed subjects. The similarity in gray matter and brain surface asymmetry maps for the SDC and YC groups attests to the validity of the methods in detecting morphological differences between hemispheres.

Results from the asymmetry analyses show that brain surface gray matter asymmetry is altered as a result of severe prenatal alcohol exposure. Results from 2 independent samples of normally developing subjects attest to the validity of these findings. The region of altered asymmetry in the ALC subjects is primarily at the conjunction of Brodmann's areas 21, 22 and 37 (Brodmann, 1909). Functional imaging studies have shown that areas 21 and 22 are primarily involved in language processing, while area 37 is involved with object and face recognition (reviewed in (Cabeza and Nyberg, 2000)). Cognitive functions subserved by these regions have been shown to be deficient in individuals with severe prenatal alcohol exposure (Church and Abel, 1998; Mattson et al., 1998). Perhaps the altered gray matter asymmetry in the ALC subjects contributes to these specific cognitive deficits. The functional imaging studies proposed by various Consortium members should also help shed more light on the functional significance of the altered asymmetry.

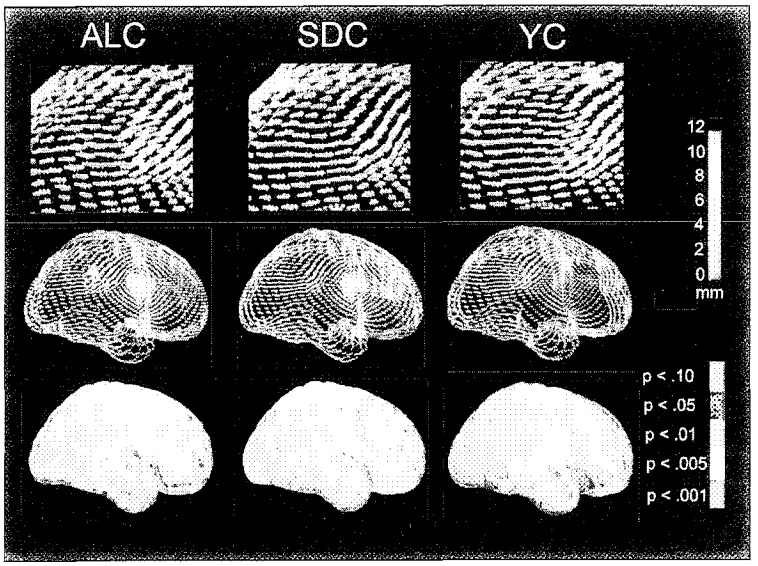

Figure 5: The arrows in these maps show the 3D direction and distance of displacement between analogous surface points in the left and right hemispheres for the average ALC, SDC and YC groups. The base of each arrow represents the left hemisphere surface point location, and the tip of the arrow represents the analogous surface point location in the right hemisphere (a flipped and reflected version). Group differences (in millimeters) are mapped in color according to the color bar on the right. Note maximal asymmetry, up to 12 mm difference between analogous surface points is found in the perisylvian region in all 3 groups, shown enlarged to enhance detail in the top row. Displacement between left and right hemispheres is primarily in the anterior-posterior axis in most regions, more prominent in the perisylvian region. Statistical maps are shown in the bottom row documenting the significance of displacement between analogous surface points in the left and right hemispheres according to the color bar (note white regions are $p > 0.10$).

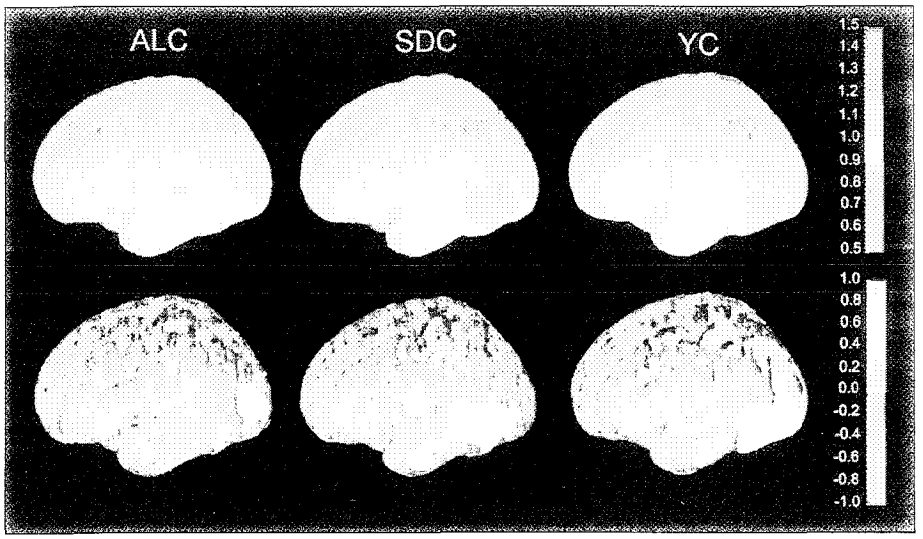

Figure 6: In the top row are ratio maps quantifying the amount of gray matter within the 15mm sphere at each brain surface point in the left hemisphere as ratio to that of the analogous points in the right hemisphere. One (color coded in green shades) represents complete symmetry. Cooler colors (greater than 1) represent regions where there is more gray matter in the left hemisphere than the right, and warmer colors (less than 1) represent regions where there is more gray matter in the right hemisphere than the left. In the bottom row are statistical maps where shades of green to yellow represent positive Pearson's correlation coefficients (regions where there is more gray matter in the left hemisphere than the right) and shades of purple and pink represent negative Pearson's correlation coefficients (regions where there is more gray matter in the right hemisphere than the left) according to the color bar on the right

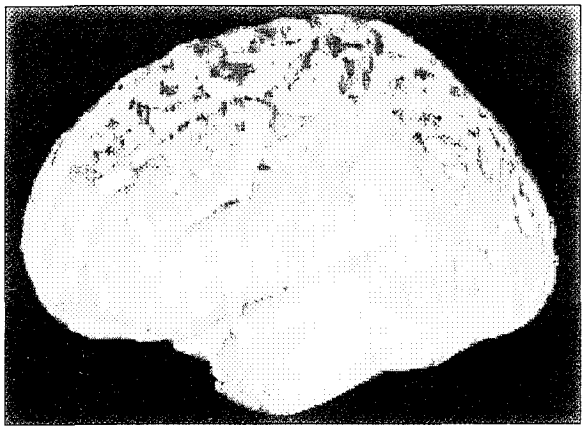

Figure 7: Statistical map of the group difference in gray matter density asymmetry. Shades of green to yellow represent positive correlation coefficients (non-significant regions where controls have more gray matter asymmetry than ALC) and shades of purple and pink represent negative correlation coefficients (non-significant regions where ALC subjects have more asymmetry than the SDC subjects). Red areas correspond to correlation coefficients that show significant decrease in gray matter asymmetry in the ALC subjects at a threshold of $P = 0.05$. Regions shown in white correspond to correlation coefficients that show significant increase in gray matter asymmetry in the ALC subjects

Results from these studies are relevant to Specific Aim 2 where we propose to improve and create automated tools for surface rendering, tissue segmentation, MR signal inhomogeneity correction, and region definition. These studies are also relevant to Specific Aim 3 where we propose to enhance tools for detailed surface analyses. All of the studies described above can be conducted with data collected by Consortium members, but significant improvement in image processing time and reliability is expected given the application of automated tools for skull stripping and tissue segmentation, which were conducted manually in the preliminary studies described above.

Summary of Surface-Based Analyses: Relevance to Proposed Consortium: Thus far, the surface based analyses in ALC subjects have shown displacements of the CC which were correlated with neurocognitive test performance. Further, the ALC subjects show increased gray matter density bilaterally in the perisylvian region with altered gray matter asymmetry in more inferior-posterior temporal lobe regions. Prominent brain shape abnormalities are also observed where the ALC subjects' brains appear to be narrower than the controls in inferior parietal/superior temporal regions with reduced surface extent in the anterior/orbitofrontal cortices. All of these effects are above and beyond the marked, global microcephaly so often observed in ALC subjects. These shape and tissue density abnormalities provide the impetus for the proposed studies because they highlight the regional nature of brain morphological differences in ALC subjects. They suggest that assessment of brain-behavior relationships may be regionally specific and that brain functional abnormalities may not be global in nature.

In order to assess brain functional abnormalities, current popular image warping algorithms (i.e., SPM99, AIR) rely on intensity-based methods and our recent results have shown that they have an accuracy for matching

sulci within only about 14 mm in some brain regions (Sowell et al., 2002b). Shown in Figure 8 are results from our recent report in normal brain development (Sowell et al., 2002b) which show sulcal variability patterns (after affine spatial normalization (Woods et al., 1993)) over the entire cortex in child, adolescent and adult populations. Notably, the regions with the greatest variability even after spatial normalization are in posterior temporal lobe regions, regions of considerable group differences in the ALC population. The results in the normally developing population highlight the lack of anatomical registration that would undoubtedly occur in these regions in the ALC subjects in these proposed functional imaging studies if we used only automated affine normalization. Following are a series of pilot studies where we have combined functional and structural data using the continuum mechanical warping algorithms where anatomical landmarks are well matched across subjects.

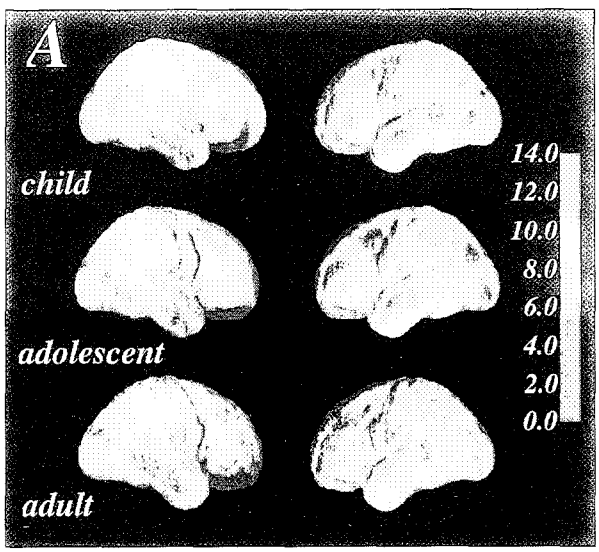

Figure 8: Cortical surface variability maps in 3D viewed from the right and the left showing variability in the average child (n=14), the average adolescent (n=11) and the average young adult (n=10). The color bar indicates patterns of variability within each group as the root mean square magnitude (in mm) of displacement vectors required to map each individual into the group average surface mesh. Note this map is representative of residual brain shape variability after affine transformation into ICBM305 standard space. Higher variability is observed in the post central gyrus and posterior temporal regions in all three age groups, with relatively less variability in precentral and anterior temporal gyri.

2) Functional Imaging Studies with Advanced Warping Strategies(Specific Aim 3)

As discussed above, diverse gyral and sulcal topography (as shown in figure 8 above) is a confound of functional studies of the human brain and is emphasized in studies involving pathology. To fully elucidate functional variability in the human brain, structural differences across subjects must be accounted for and removed during the analysis. Intensity based registrations limit much of the anatomic variation, but they have flaws. Large deviations between the source and target brain morphology will not be corrected due to an inability of an automated approach to identify anatomy. Using anatomic landmarks from structural MRIs and a high-dimensional continuum mechanical warping algorithm from Thompson et al.,(Thompson and Toga, 1997; Thompson et al., 2000b) we have aligned functional scans from neurosurgical patients and analyzed how the location of a mass affects activity in an fMRI study of tongue movement (Rex et al., 2001). Similar analyses were conducted for FAS and control subjects in a separate study where the activation paradigm tapped "higher" cortical functioning, specifically frontal lobe response inhibition in a go-no-go task.

Cortical Surface Matching for Improved Detection of Functional Activity: Tongue Movement in Tumor Patients:
Eight patients with left hemisphere pathologies (3 frontal masses, 1 frontal hemangioma, 3 temporal masses, and 1 temporal AVM) and no language dysfunctions were chosen for a full brain structural MRI and fMRI of tongue movement. Structural scans were T1-weighted SPGR MRIs (0.9375x0.9375x1.2mm^3 voxels) taken on a 3T General Electric in the sagittal plane. They were aligned to Talairach space with a 7-parameter transformation, global scaling constrained by AC-PC distance, RF corrected using the N3 correction scheme (Sled et al., 1998), and parametric cortical surface meshes were extracted (MacDonald et al., 1994). Landmarks were delineated on every cortex from the sulcal anatomy and used to drive the continuum mechanical registration of the structural scans (Thompson et al., 1997). Functional scans were acquired by a gradient echo planar imaging sequence in the axial plane (3.2x3.2x4mm^3, 1mm gap). They were motion corrected and aligned to the corresponding structural scan via rigid body transformations using the Automated

Image Registration suite (Woods et al., 1998a). Each fMRI was analyzed by correlating voxel intensity changes with a pre-determined hemodynamic response (Bandettini et al., 1993). Results were thresholded at $p < 0.001$ to generate activation maps and projected up to 6mm onto the cortical surfaces to show activity for cortical gray matter. The structural warping fields drove the cortical activity maps into anatomic alignment and functional probability maps were created. Comparisons were made between left and right hemispheres using all the patients and between temporal mass patients and patients with frontal or parietal lobe masses.

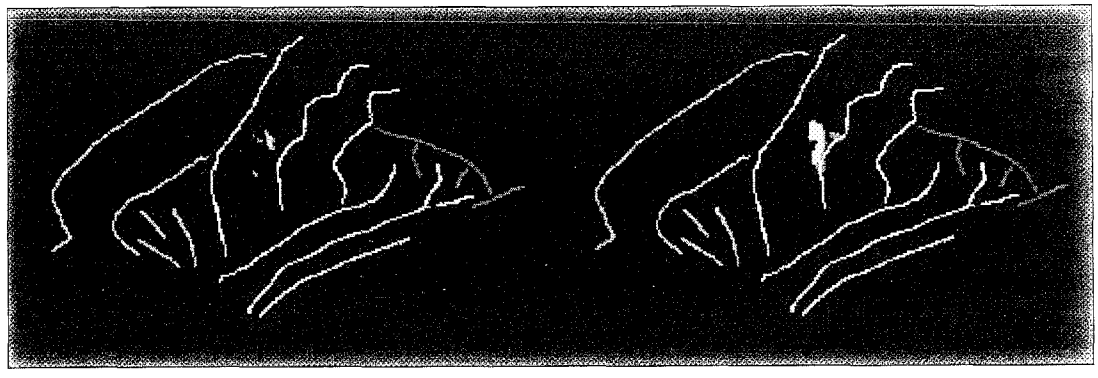

Figure 9: Only the patients with temporal lobe masses were used in this comparison in order to best avoid the confound of the effect of the pathology on observed functional activity. The improvement in the localization of activations across the group can be seen in the flat sulcal maps of the left hemisphere shown in the above figure. The Talairach alignment with surface projection is shown on the left. The sulcal lines are in the average position for the group. The paucity of activity seen, 10.8mm^2 of overlap for the entire group, is located on the pre-central gyrus. This is normally consistent with expectations for the localization of motor activity, but in fMRI there is usually a pronounced sulcal effect that is lacking here. The alignment on the right side of the figure uses the additional continuum mechanical warping step to place all the anatomy in register at the gross level allowed by a structural MRI resolving 1mm^3 voxels. The overlap of activity for the group is now measured to be 45.0mm^2; over 400% greater than without the high-dimensional warping. Furthermore, the sulcal anatomy projected on the activity map is now known to be in precise register with the underlying map. It is now seen that the activity does have a strong adjacent sulcal component, as would be expected, along with the pre-central gyrus activation caused by the tongue movement paradigm.

Cortical Surface Matching for Improved Detection of Functional Activity: Response Inhibition in FAS and Control Adolescents: Two FAS (ages 16 and 18 years) and one control subject (age 16 years) underwent fMRI and high resolution structural MRI in San Diego (with Dr. Edward Riley, the PI of the Administrative Core of the proposed Consortium). The activation paradigm was a blocked design go-no-go task and the contrast of interest was go vs no-go tapping frontal response inhibition functions. The same image analysis methods described for the tongue movement paradigm in tumor patients were utilized here. Functional images were aligned to the hi-resolution structural images; activation maps (go vs no-go) for each individual were created using SPM99 (Friston et al., 1995) and a height threshold of $p = 0.07$; the structural warping fields (based on anatomical sulcal landmarks) drove the cortical activity maps into anatomic alignment; and functional probability maps were created where we assessed for overlap in functional activity in all 3 subjects. Given findings from earlier studies (e.g. (Konishi et al., 1999)), we expected activation in the right inferior frontal lobes more prominent in the no-go than the go condition. Results are shown in Figure 10. As expected, we do see common activation in right inferior frontal cortex which is significant at a probability of .0003 (uncorrected) according to a binomial probability density function (i.e., 3 subjects overlapping activation with an individual probability threshold of .07). The activation common to all 3 subjects is scattered outside the expected area as well around the anterior frontal lobes, and the expected right inferior frontal activation is more on the orbital surface of the brain than would have been expected from the earlier studies of response inhibition (Konishi et al., 1999). Nonetheless, these results highlight the necessity for using high-dimensional warping strategies. Note the displacement of activation when images were averaged using intensity based affine registration as compared to the high-dimensional warping algorithms. Note also the size of the cluster in the inferior frontal lobe where we predicted activation in this paradigm is larger in the high-dimensional warped average (109 mm^2) than in the average created from affine registration (52 mm^2). Together, these findings indicate that we would infer incorrect localization of functional activation, and underestimate the magnitude when relying solely on traditional intensity-based affine registration as employed in most functional imaging studies.

As shown in Figures 9 and 10, these new techniques for characterizing functional activity across a group allow greater discriminating power in studies of population differences. The ability of the high-dimensional warps to align like regions of anatomy will allow the functional locations and variability of activity to be characterized with more accuracy and precision which is of critical importance when brain shape differs between groups as it does in the FAS population. Further, the preliminary studies of FAS subjects illustrate that we are capable of using the cortical matching strategies with less robust (less robust than activation observed in a tongue movement paradigm) higher cortical functional activation paradigms such as those we propose to use here. They also illustrate that subjects such as the ones we plan to recruit for these proposed studies can tolerate the fMRI and structural MRI procedures.

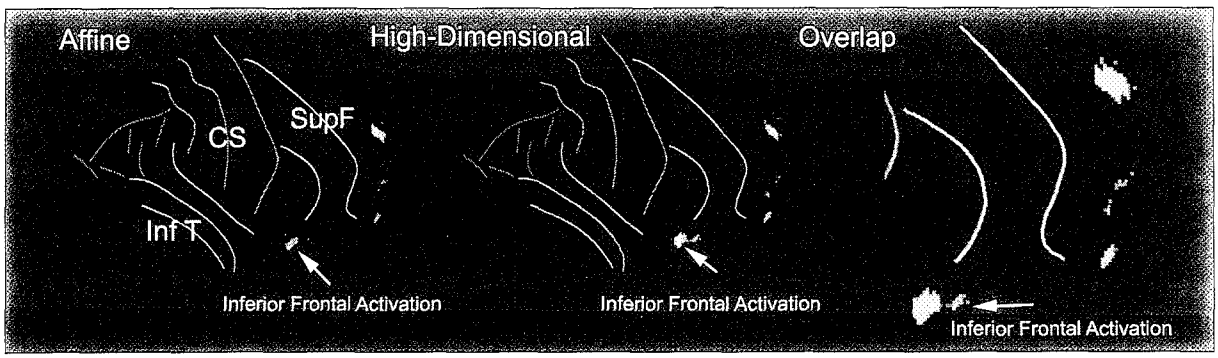

Figure 10: Only significant activations that fell within the frontal lobes are shown here on these right hemisphere flattened brain surface maps. Activations in the affine average are shown in red, and in the high-dimensional average are shown in green, with the overlap between the two shown in blue in the image on the right. The improvement in the localization of activations across the group can be seen in the flat sulcal maps of the right hemisphere shown in the above figure. Frontal lobe sulci are shown in yellow, central, pre-central and post-central in purple, occipito-parietal in dark blue, and temporal lobe sulci are shown in light blue.

The fMRI statistics are currently estimated from a general linear model (Friston et al., 1995), but we will be able to assess tissue loss rates, and gray matter thickness estimates, as attributes in parameter space for covariation with activation data. This will help us identify structure/function relationships in the FAS subjects, and will help build joint statistical tests (based on structure and function) for detection of deficits.

Summary of Functional Imaging Studies with Advanced Warping Algorithms: Relevance to Proposed Studies: Preliminary studies where surface-based warping algorithms have been used to match anatomy across subjects have been fruitful in 1) demonstrating that the techniques can actually be applied to image data similar to what Consortium members propose to collect, and 2) that the detection of functional signal differences between groups, or averages across groups is considerably improved over more traditional image averaging typically used in functional imaging studies. These preliminary studies are directly relevant to Specific Aim 3 where we propose to adapt tools for combining functional and structural imaging information. As part of the Imaging Core, we will create algorithms to link maps and patterns of structural differences, or brain change, with functional or cognitive deficits mapped in the same subjects. New flattening and matching approaches applied to cortical regions will elucidate structure/function relationships with previously unobtainable resolution. Nonlinear elastic matching approaches (Thompson et al., 2000b; Thompson et al., 2001a) will be engineered and optimized to compare and integrate functional activation data across subjects, and relate functional features to underlying anatomical deficits. All of these advanced image analysis methodologies will be made available to Consortium members who collect functional and/or structural brain image data.

3) Brain Shape Correlated with Other Types of Data (Specific Aim 4)

While we have not conducted statistical analyses for correlations between brain surface dysmorphology and behavioral measures in the ALC subjects, we have conducted these studies in a group of children with attention deficit hyperactivity disorder (ADHD) (Sowell et al., Submitted). We believe these studies illustrate

well the means by which we propose to correlate structural image data, with the disparate data collected by other projects in the Consortium.

In this study, we used high-resolution MRI and surface-based, computational image analytic techniques like those described above in the ALC subjects to map correlations between subject's scores on measures of attention and hyperactivity and anatomical features at the cortical surface in a group of 27 children and adolescents with ADHD and 46 age- and gender-matched control subjects. As predicted, abnormal morphology was observed in the frontal cortices of ADHD subjects, with reduced regional brain size localized primarily to inferior portions of dorsal prefrontal cortices bilaterally. The correlation maps for DFC and the 2 behavioral measures (i.e., inattention and hyperactivity) within the ADHD and control groups were also generally unremarkable, with one exception. Within the ADHD group, permutation tests revealed trend level significant positive correlations between DFC in the dorsal frontal region in the left (P = 0.065) and right (P = 0.056) hemispheres. Assessment of the statistical map in Figure 11 reveals regions in the mesial dorsal frontal cortex where ADHD subjects with greater brain surface extent (i.e., larger mesial dorsal frontal regions) tended to have higher hyperactivity scores on the ADHD rating scale. While only at trend level significance, these results are intriguing given the role of frontal cortex in ADHD and in response inhibition (hyperactivity) which is deficient in ADHD subjects.

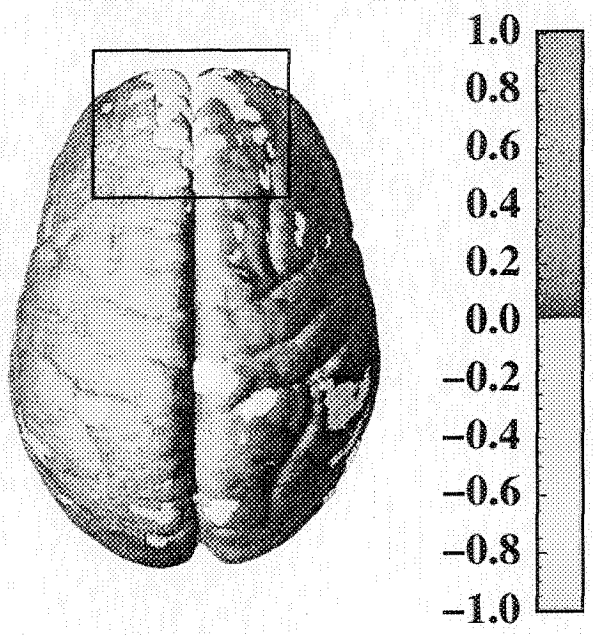

Figure 11: Correlation maps between DFC and hyperactivity scores within the ADHD group (top view) showing the significance of these correlations according to the color bar on the right (Pearson's correlation coefficients ranging from –1 to 1). Regions overlaid in white represent positive correlations where increased DFC is associated with elevated inattention scores. Note the large white clusters surrounding the interhemispheric fissure in the dorsal frontal cortex, shown within the black square.

D. Research Design

Overall Research Design: In this study we propose to refine and validate brain image analysis tools for analyzing structural and functional magnetic resonance imaging data collected by the various Consortium sites. We plan to assist consortium members with image acquisition protocols, calibrate scanner profiles to enable data combining, disseminate image analysis tools, use more innovative image analysis tools within LONI, and aid in correlational studies combining imaging data with data collected by other Consortium Cores. These projects will be carried out on data from approximately 780 children and adolescents (FASD and control subjects) scanned by 4 Consortium sites over the 5 year funding period (see Table 1).

Table 1: Proposed Image Data							
Number of Subjects FASD (control)							
	Scan Type	Year 1	Year 2	Year 3	Year 4	Year 5	Magnet
San Diego	sMRI fMRI	50(20)	20(20)	20(20)	20(20)	20(20)	1.5 Tesla
Moscow	sMRI	40(30)	40(30)	40(30)	40(30)	40(30)	.4 Tesla
Atlanta	sMRI	3(2)	5(5)	5(5)	5(5)	2(3)	3 Tesla
Los Angeles	sMRI fMRI	10 (10)	20 (20)	10 (10)	0	0	1.5 Tesla
Finland	sMRI MRS	0	20(0)	20(0)	20(0)	0	1.5 Tesla
Total		165	180	180	140	115	
				Grand Total (upper estimate)			470(310)

Archival and Data Base: Data will be transferred from interested participating sites via internet file transfer protocol (ftp). Data can also be transferred via CD through regular mail. Archival and database for data collected as part of this Consortium is essential to ensure that the value of the data collected is retained throughout the analytic process and its interpretation. The data must be accessible and secured and multiple copies will be created at different sites. The objective of our archival and backup systems work to absolutely ensure the integrity and accessibility of data throughout the project and into the future. Systems that have been devised at LONI include the following schedules. Incremental backups where any data that has been modified, created or altered in any way are performed on a nightly basis. Backups include copy of all these data to our DLT offline systems, as well as the hierarchical storage systems contained within the StorageTek robot. All data that is created at any time is created in multiple copies. Disk copies are created for immediate access and mirrored volumes are established on the SotrageTek system. Multiple tape copies contained within the StorageTek are exact duplicates of each other. Weekly incremental backups are also created such that copies of the dailies may also be residing on the weekly backups. Finally, monthly full backups of the entire system are performed automatically within the StorageTek system.

A LONI Image Database has been constructed for other large multi-site collaborative projects in the laboratory, and a similar system will be utilized for data collected as part of the CIFASD. The data base provides an effective means for archival and protection of collaborator collected image data. The goal of this software is to provide a convenient mechanism for searching the existence of particular image data while protecting its usage at the same time. We will build the appropriate database query mechanisms to ensure that no image data or identifying patient information will be accessible to the outside world or to any others without the appropriate authorization. The LONI Database will provide a convenient mechanism for backup and security so that data will not be compromised nor exposed to catastrophic loss with equipment or disk failure. Further, the LONI Database will provide a convenient input mechanism for pipeline processing. Image collections created within the LONI Database can be directly fed into the LONI pipeline environment (see Dissemination section below) for processing and analysis.

Specific Aim 1: "Image Acquisition Calibration: We will scan a human volunteer and a mechanical phantom on all magnets that will be used to collect structural MRI data in order to establish the protocols and parameters for scanner calibration to correct scanner-specific geometric distortion. In order to calibrate data collected from each scanner, we will calculate the deviation in spatial registration between phantom (human and mechanical) images collected at each site, and apply spatial correction algorithms to ensure that they are anatomically (and geometrically) matched. We will work with other Consortium members to help them best perfect their image acquisition protocol that may vary somewhat by magnet manufacturer."

The UCLA Laboratory of Neuro Imaging has considerable experience in coordinating and participating in multi-site data collection collaborations (e.g., Computational Anatomy and Multidimensional Modeling, NCRR 2P41RR013642-05; International Consortium for Brain Mapping, ICBM, P01 MH52176; Biomedical Informatics Research Network, Brain Morphology BIRN, 02076682 (M01 RR00827)). We will capitalize on software algorithms developed for scanner calibration and geometric distortion correction developed under those

projects, and have modeled our human and mechanical phantom studies for this Consortium Imaging Core after these large multicenter image acquisition projects. Following is a summary of our planned activities.

Phantom studies: Image acquisition distortions and signal fluctuations may be imposed by any of the magnets of various Consortium members. Correction of geometric distortion can be made with a uniform set of linear, nonlinear and local deformation parameters applied to each subjects' data set depending on which scanner was used for acquisition. Corrections for signal contrast differences can be made with an image intensity scaling factor obtained for each scanner. We propose human and mechanical phantom studies with the goal of minimizing errors and variance introduced by the structural image acquisition process and to ensure that data collected from various sources can be directly compared. Of course this added complexity of phantom studies could be eliminated at the outset, by restricting support from the Imaging Core to those sites with a particular scanner vendor and field strength, but this would severely reduce access to a diverse FASD population.

Mechanical Phantom: We will use a specially designed cylindrical phantom (from Data Spectrum Corporation) that has fiducial holes in a regular geometric pattern where each fiducial is separated by 10 mm from its nearest neighbor (see Figure 12). As seen in the MR image of the phantom, geometric distortion is relatively subtle when imaging with a 1.5Tesla magnet, and cannot be visually detected. This regular geometric grid will also be helpful in validating the subtle correction algorithms because the theoretical correct result is known. This phantom will be transported to each magnet and scanned with the T1-weighted image acquisition protocol selected at each site. The actual distortion at each point in space can be calculated by assessing the deviation of the actual phantom from the expected, real coordinate measurements by using automated registration algorithms (Woods et al., 1998a; Woods et al., 1998b). The distortion parameters can then be applied to each scanner specific image data set prior to any other image analyses.

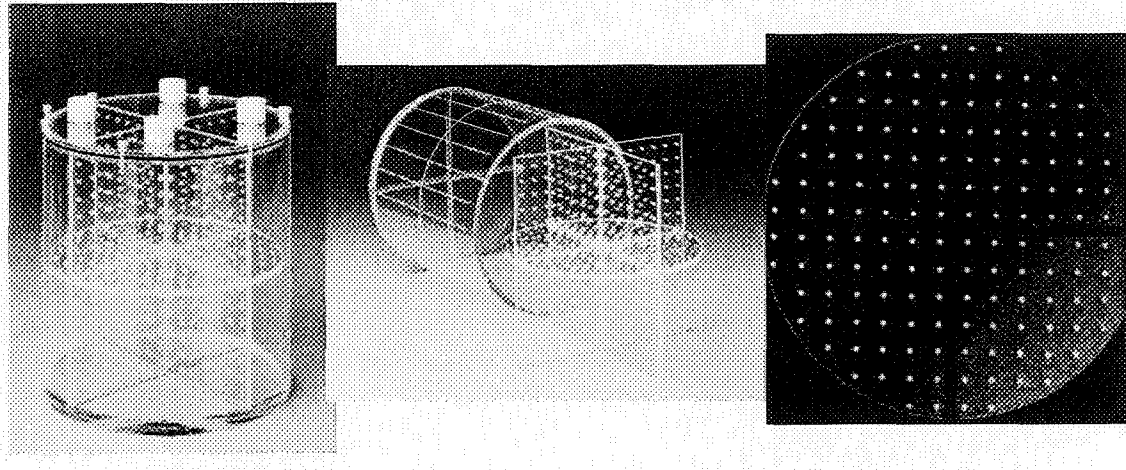

Figure 12: Data Spectrum Corporation's geometric 3-dimensional cylindrical phantom photographs, and T1-weighted image axial slice through the center (right). The phantom will be placed in each scanner, and imaged with the T1-weighted acquisition protocol selected for each site.

Human Phantom: The human "phantom" will allow us to address the validity of correction factors derived from the mechanical phantom described above. While tissue contrast and overall signal value may vary as a function of the scanner being used, the morphology of the brain of the same individual will remain constant. Spatial differences between images of the same individual scanned on separate scanners should be minimal after correction for geometric distortion. Displacement can be quantitatively assessed by selecting anatomical landmarks throughout the brain volume, and assessing the average distance between points as a function of scanner. While other factors which introduce noise will be present (i.e., reliable selection of anatomical points) the noise introduced by the scanner should not be greater than the noise introduced by anatomical rater accuracy.

The human "phantom" will also allow us to equalize signal value and tissue contrast across scanners. Recent research has shown that the aggregation of MRI data from various centers should not be done without correction for geometric distortion (as described above) and partial volume averaging (depending on image acquisition orientation) (Patwardhan et al., 2001). Doing so can result in unstable anatomical volume

measures which are scanner dependent (Filippi et al., 1997). These problems can be addressed with correction algorithms derived from geometric phantom studies and repeat scanning of individuals on various magnets. Various methods, such as histogram matching (Wang et al., 1998) have been used to ensure that signal intensities for different brain tissues are similar for the same individual scanned with similar imaging protocols on different magnets. Similar methods have been used in our other large multicenter image acquisition projects (FIRST BIRN, ICBM).

Scanning Procedure: Difficulties arise when trying to assure quality control by using mechanical phantom studies. The projects proposing imaging studies in this Consortium are geographically widely dispersed (US, Russia, Finland), and reasonable concerns would arise about shipping the phantom from imaging site to imaging site (i.e, was it received? Was it damaged in shipment?). Further concerns result from correct placement of the phantom in each site's magnet. We propose a more reasonable solution in this proposal which is to have the same individual who will be the "human phantom," transport the mechanical phantom during travel to all the Consortium imaging sites. This person will most likely be one of the Consortium investigators who will be required to travel to all imaging sites as required by other cores (i.e., dysmorphology core, administrative core director). This individual will be trained on how to place the phantom in the magnet. This approach seems reasonable also given exorbitant travel costs of sending a technician to the various international sites.

Image Acquisition Protocol: Final MRI pulse sequence specification will be determined during the earliest phase of funding. From our past experience with state-of-the-art image analysis algorithms (see Preliminary Studies), we anticipate that a high-resolution 3-dimensional T1-weighted series will best accommodate our image analysis proposal. The image data will be collected with voxel dimensions of approximately 1 by 1 mm within the sagittal plane (plane of acquisition), with a TR of 24 ms, TE=5 ms, NEX=2, flip angle=45 degrees, field of view of 30 cm, 124 slices with section thickness of 1.2 mm, no gaps. This protocol takes approximately 19 minutes of imaging time at 1.5 Tesla, and a similar protocol is expected to take less time at higher field strengths. Variations in this protocol are to be expected given different scanner manufacturers and varying field strength. Pilot data (scans of the investigators themselves) can be transferred to LONI via ftp, and imaging parameters for subsequent scans can be altered as a result of image inspection by the Imaging Core investigators until the exact protocol for each image acquisition site is perfected.

It is anticipated that some projects in the Consortium may not have the resources to dedicate to such high resolution structural imaging data. Some image analysis procedures can be performed with lower resolution images. The most global analysis proposed to be conducted by all imaging sites is measurement of the corpus callosum in the midline sagital plane. A much shorter imaging time is required for a similar protocol with NEX = 1 (about 9 minutes), and will yield images comparable (though suboptimal) to the higher resolution data, adequate for automated CC measurement.

Specific Aim 2: "Automated Tools for Distribution: We will adapt automated image analysis tools for dissemination to the various sites collecting structural brain imaging data to assess CC shape and other brain structural information. All software adapted and created for the purposes of this Consortium will be platform independent, and user-friendly. The Imaging Core will provide training via web-based, in-person and email supported mechanisms on the use of the tools, and conduct shape analyses on the CC contours provided by the various imaging groups within the Consortium."

Automated Tissue Classification/Skull Stripping/Surface Extraction: We have developed several methods for automated analysis of T1-MRI data. These include extraction of the brain from the skull and scalp, correction of RF artifacts in the extracted brain volume, classification of the tissues within the brain volume, and generation of topologically consistent surfaces from the classified brains. We produced these tools as stand-alone command line programs that execute on a variety of platforms (SGI Irix, Sun Solaris, Linux, Microsoft Windows, Apple Macintosh OS-X) and as a single interactive tool named BrainSuite (Shattuck and Leahy, 2002). These tools are publicly available and can be used locally by investigators downloading the files onto

their own computer systems, or remotely through the LONI Pipeline, described in more detail below. The graphical user interface and brain surface extraction methods of BrainSuite are illustrated in Figure 13.

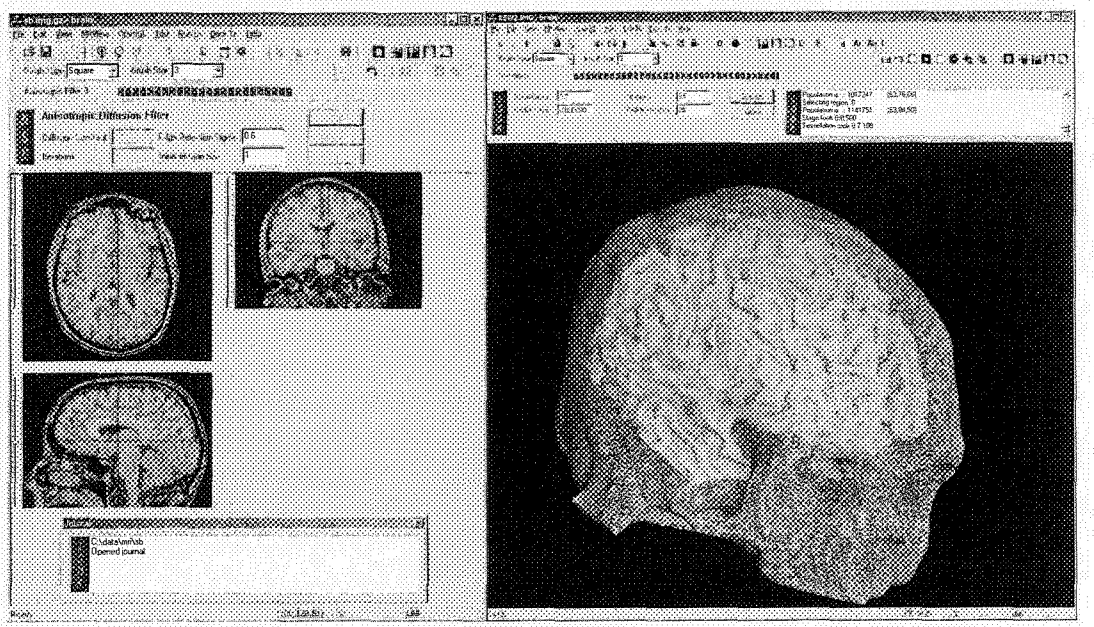

Figure 13: The BrainSuite surface identification tools in (left) orthogonal MRI display mode and (right) surface display mode.

The Brain Surface Extractor (BSE) (Shattuck et al., 2001) extracts the brain from the skull and scalp using a combination of anisotropic diffusion filtering, Marr-Hildreth edge detection, and mathematical morphology. The anisotropic diffusion filter preserves strong edge content within the brain volume while smoothing small local tissue differences. This improves the result of the edge detector, which generates contours within the filtered MRI volume. One of these contours is the boundary between the skull and scalp, which will generally leave the brain intact as a connected component. This contour will be interrupted by small chains of voxels as a result of natural features such as the optic nerves, noise artifacts, or the limited resolution of the scanner. To sever these connections, we apply a sequence of morphological operations. First, we apply an erosion operator; this will break any features that are the size of the erosion element. Then, we identify the connected components within the image and automatically select the one corresponding to the brain. Though the largest component will usually be the brain, we test the centroid and mean value of the region to ensure that we do not select a large connected component corresponding to background voxels. We then restore the brain to its original size by applying a dilation operation, followed by a closing operation that fills surface pits that may result from edge mislocalization.

The Bias Field Corrector (BFC) software (Shattuck et al., 2001) uses a parameterized tissue model to estimate local intensity variations due to RF artifacts. First, we produce a set of global estimates of mean tissue intensities for WM, GM, and CSF based on automated histogram analysis. These estimates are used in a mixture density model that includes parameters for tissue intensity, local intensity gain, and tissue composition. We then analyze the histograms of a set of regions spaced throughout the brain volume. We assume that the gain field is smoothly varying and model the gain as a local constant for each region. We then fit the model to the histogram of the region, which produces an estimate of the gain for that region. We process these estimates to remove outliers, and then fit a tri-cubic B-spline to the remaining estimates. The spline estimates the values for the non-uniformity for every voxel in the brain volume; we divide this estimate out of the image to remove the non-uniformity.

The Partial Volume Classifier (PVC) (Shattuck et al., 2001) produces a labeled estimate of the non-uniformity corrected brain volume (i.e., tissue segmentation). PVC uses the same measurement model as BFC, but with the gain parameter set to unity for the entire image. We formulate a *maximum a posteriori* classifier using a

spatial Gibbs prior. This prior penalizes dissimilar label configurations, such as white matter (WM) being directly adjacent to gray matter (GM). PVC can be used to produce three-class (GM,WM, and CSF) labelings or six-class labelings that also identify partial volume combinations of tissue types within the image. These label volumes can be used to study various brain attributes, including composition of specific regions, or as a basis from which to generate anatomical surfaces that model cerebral structures.

We produce surface models of brain structures using the Marching Cubes algorithm (Lorensen and Harvey, 1987) applied to binary regions identified from the tissue labeled volumes. These regions can be identified using interactive tools such as BrainSuite. For example, BrainSuite includes tools to simplify the extraction of the cerebral WM from the rest of the brain volume. We are currently developing automated approaches that use registration techniques (Woods et al., 1998a; Woods et al., 1998b) to identify a structure to be tessellated.

Surfaces produced by Marching Cubes from tissue-classified volumes will typically exhibit numerous topological handles on the surface, which correspond to segmentation errors or limitations of the resolution of the MRI relative to the features of the neuroanatomy. To address this problem, we developed a novel method for constraining the topology of a binary volume to produce tessellations that are equivalent to a sphere (Shattuck and Leahy, 2001). This method analyzes the binary volume using a graph-theoretic approach. It identifies sets of voxels that are either removed or added to the volume to break handles or fill holes. With spherical topology, these surfaces can be parameterized using a two-dimensional coordinate system. We can produce such a parameterization by deforming the surface into a sphere using a set of applied forces.

Adaptive Elastic Segmentation: We propose to distribute fully automated software for segmentation of the corpus callosum. This software, developed at LONI (Pitiot et al., 2002), applies a combination of elastic template matching and an evolutionary heuristic. The purpose of the software is to retrieve the boundary of a brain structure automatically from MR data (see Figure 14). The approach is to fit a series of deformable templates to the target contour such that the template is modeled using a parametrized curve whose coefficients are iteratively updated to minimize an objective function (such as the contour of the corpus callosum in the midsagittal plane). The evolutionary heuristic is used to control the behavior of the various templates (i.e., the corpus callosum template) by 1) incorporating statistical constraints to bias the deformation toward a range of shapes derived from a statistical analysis of a learning set (i.e., a series of callosa manually defined in existing LONI data sets), and 2) selecting and favoring the most promising templates at each round. More geometrically complex brain structures (i.e., the caudate nucleus) can also be automatically defined using this adaptive elastic segmentation paradigm. The software requires 1) initial positioning of the deformable template with respect to the target structure, 2) use of a priori statistical information about the shape of the target structure (provided from existing data sets analyzed at LONI), and 3) the final search for a global solution in a computationally effective fashion. Comparisons between the automated segmentation and expert manual segmentation were favorable, attesting to the validity of the method (Pitiot et al., 2002). The adaptive elastic segmentation software will be compiled to function on MacIntosh and PC computers, and will be supported by LONI staff to enable Consortium members to define the callosa, or other brain structures in the MR image data sets they collect. Use of the software will also be supported through the LONI Pipeline (see Dissemination section below) which allows consortium members to access LONI and its resources remotely. Statistical analyses of callosal shape and size dysmorphology can then be assessed using the methods described in the Preliminary Studies.

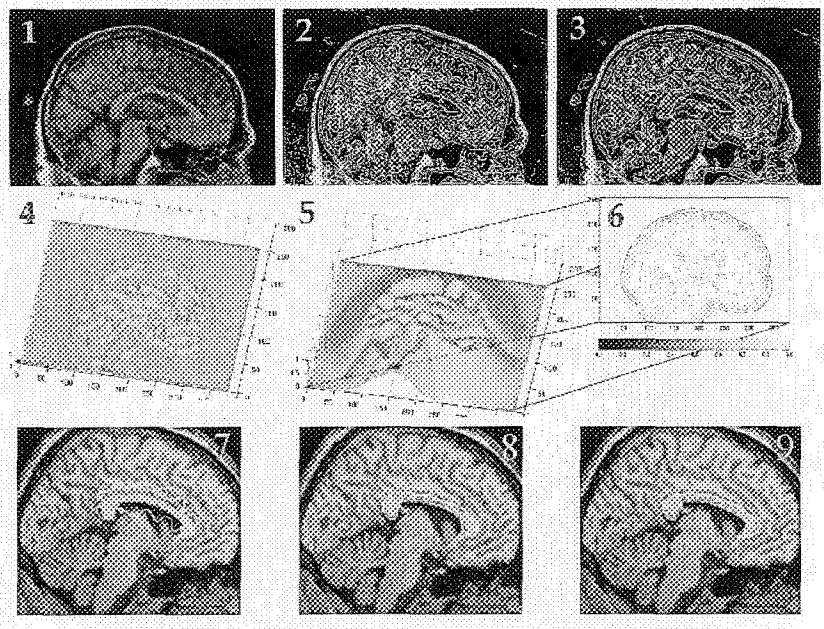

Figure 14: Adaptive Elastic Segmentation: A prototype template, in the form of a B-spline, is warped in a potential field which guides the deformable contour. In contrast to prior approaches, the potential field is adapted both spatially and temporally. This improves the speed and accuracy of the object extraction process. The potential field is initially designed based on spatial characteristics of edge features in the input image. This guarantees efficient dynamics as early as the first iterations. The potential function, which guides the deformable contour, is also logarithmically re-mapped to improve the global consistency and convergence speed of the evolution process.

Adaptation, Improvement and Creation of Automated Image Analysis Tools: All of the automated image analysis tools described above are fully functioning, and available online to the neuroimaging community. For the purposes of this Consortium, significant improvement of some of the existing tools and creation of new tools is planned which will enhance our ability to investigate brain morphological abnormalities and neurobehavioral correlates in FASD. Some of the image analysis tools used in our previous studies have been created by other research groups (i.e., brain surface rendering, tissue segmentation), which limits our flexibility in creating new image analysis strategies. The tools developed within LONI, with some planned modification and improvement, will make the software developed by other research groups obsolete and allow us the ultimate flexibility to design image analyses specific to the Consortium's research questions. Specifically, we plan to do the following: 1) Develop a novel method for surface parameterization that will allow surface models generated by BrainSuite to be used in statistical analyses of brain surface features (i.e., gray matter density, local brain size) and correlations with data collected by other projects and cores. This method will analyze the connectivity of the surface meshes, which are restricted to spherical topology, to induce a 2D coordinate system on the mesh. This method will allow parameterization of various anatomical surfaces, including cerebral cortex and face models. 2) Develop software to assess cortical thickness (in millimeters). This method will replace the cruder measures of gray matter density, and will instead compute cortical thickness from the GM/WM surface and the tissue-labeled brain volume. The distance from the inner surface to the outer boundary will be computed, producing an estimate of GM thickness at each point on the high-density surface. 3) We will improve our Bias Field Corrector (BFC) to ensure that it is robust with the various image acquisition protocols utilized by various research projects within the Consortium. We will modify BFC to use a multi-resolution approach. BFC will first correct large-scale artifacts that can be estimated more robustly than smaller scale artifacts, and then correct artifacts of decreasing spatial scales. 4) We will create new tools specifically designed to identify surface models of the face from the MRI data. These tools will be based on our prior work on whole scalp identification (Dogdas et al., 2002), but will provide parameterized surface models specifically of the face. We will make use of curvature analysis to identify crest lines on the face that correspond to important facial features.

Dissemination: The use of basic image analysis tools by consortium members will be greatly facilitated by the Laboratory of Neuro Imaging (LONI) pipeline (Rex et al., In Press). The analysis of raw data in neuroimaging has become a computationally entrenched process with many intricate steps run on increasingly larger datasets. Many software packages exist that provide either complete analyses or specific steps in an analysis. These packages often possess diverse input and output requirements, utilize different file formats, run in particular environments, and have limited abilities with certain types of data. The combination of these packages to achieve more sensitive and accurate results has become a common tactic in brain mapping

studies but requires much work to ensure valid interoperation between programs. The handling, organization, and storage of intermediate data can prove difficult as well. The LONI Pipeline Processing Environment is a simple, efficient, and distributed computing solution to these problems enabling software inclusion from different laboratories in different environments. Basically, the LONI pipeline allows use of LONI software and computing resources from off-site with a user-friendly GUI interface (see Figure 15). The goal of the LONI Pipeline Processing Environment is to provide a cross-platform, distributed environment for the design, distribution, and execution of brain mapping analysis protocols. It is engineered to be intelligent, efficient, simple, and flexible. The environment was developed with the aim of greater access to various techniques, algorithms, programs, and computing power. The improvements in interoperability can facilitate collaboration between developers of specific tools and cooperation among those with unique datasets. The LONI Pipeline Processing Environment makes studies with a very large number of subjects more obtainable. It enables a high degree of sensitivity and accuracy by supporting the mixing and matching of programs from various packages developed in different laboratories. It is designed for maximum portability and platform independence. It will run on any system with a Java Virtual Machine of version 1.3 or newer. When a client logs into a Pipeline Server they are presented with all the modules, pipelets, and full pipelines the server can run. The client user can immediately select a pipeline from the server, load it with data, and execute it on the server. Alternatively selected modules or pipelets from the client and the server can be connected together. These complex pipelines can be saved in the user's module listing and recalled for later use. Server based pipelines and pipelets may only be accessed when the user is connected to the appropriate servers. When server modules or pipelets are executed their inputs are transferred to the server and the underlying modules are placed in the server's launch queue for execution. When completed, outputs are transferred back to the client only if they are explicitly saved or needed for a client module to run. Multiple server connections are allowed in a pipeline session. Modules and pipelets may be mixed from many different servers in a single workspace. The client will act as a master to all the connected servers and dictate all the file transfers and module launches that are to occur. If files are provided to the pipeline through URLs, the client or appropriate server will download them for use by the appropriate module. The LONI pipeline is currently used by many LONI collaborators through the BIRN project (Biomedical Informatics Research Network, Brain Morphology BIRN, 02076682 (M01 RR00827) and the LONI Resource (Computational Anatomy and Multidimensional Modeling, NCRR 2P41RR013642-05), and is integral in disseminating software to our numerous national and international collaborators.

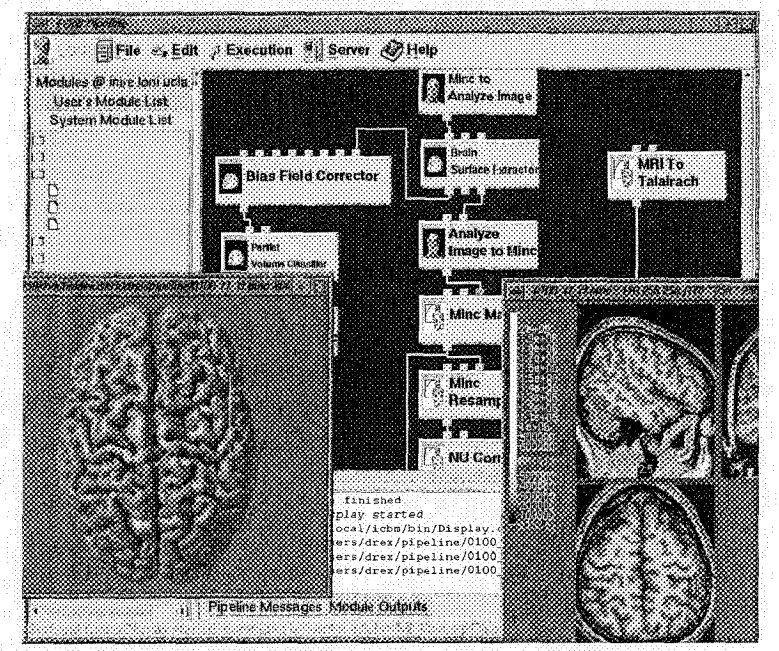

Figure 15: The LONI Pipeline Processing Environment is a visual programming interface for the simplified design, execution, and dissemination of neuroimaging analyses. Modules can be added, deleted, and substituted for other modules within a pipeline analysis. The environment handles bookkeeping and information transfer between modules and within a pipeline. Its Java based design and client/server abilities provide a platform independent solution to the interoperation of various modular packages for image processing in brain mapping (Rex et al., In Press).

Support of Automated Tools: Technical support for the automated tools and use of the LONI pipeline will be conducted via telephone, email, and existing/adapted web-based instruction and feedback methods.

Specific Aim 3: "Adapted Tools for Detailed Surface Analyses: We will create and adapt more sophisticated tools to be used within LONI applied to structural imaging data collected at various sites. Further, we will adapt tools for combining structural and functional MRI data for those sites collecting these types of imaging data. These tools will be used to assess brain dysmorphology in cortical and subcortical brain regions of interest, and to account for structural variability when assessing functional signal using MR spectroscopy or functional MRI. In this instance, it is envisioned that imaging data from all interested participating sites would be transferred to LONI where dedicated staff would conduct image and statistical analyses under the supervision of the Imaging Core PIs, and in collaboration with the consortium members collecting the imaging data."

Structural Image Analysis: Image processing for the structural data sets will be similar to those described in our earlier studies (Sowell et al., 2001b; Sowell et al., 2002a; Sowell et al., 2002c) and described above in the preliminary studies. However, we plan to rely more heavily on the automated preprocessing tools (i.e., BSE, PVC, BFC) being adapted as Specific Aim 2 of the Imaging core of this Consortium. Briefly, image analysts will conduct a series if pre-processing image analytic steps including tissue segmentation, skull stripping, and automated surface rendering. Then, image analysts who will be blind to subject diagnosis, gender and age will draw 3D models representative of 17 sulci (Sylvian fissure, and central, pre-central, post-central, superior temporal sulcus (STS) main body, STS ascending branch, STS posterior branch, primary intermediate sulcus, secondary intermediate sulcus, inferior temporal, superior frontal, inferior frontal, intraparietal, transverse occipital, olfactory, occipito-temporal, and collateral sulci) in each hemisphere on the surface rendering of each subject's brain. Points on the cortical surfaces surrounding and between the sulcal contours drawn on each individual's brain surface will be calculated using the averaged sulcal contours as anchors to drive 3D cortical surface mesh models from each subject into correspondence. This type of analysis is known as high-dimensional continuum mechanical image warping (Thompson et al., 2000a; Thompson et al., 2001c). This allows the creation of average 3D surface models for the alcohol and control groups, and the creation of group average maps of various features of the brain surface such as local brain growth or brain shape and gray matter density as described in the preliminary studies, and described in more detail below in the "Functional/Structural Image Analyses Combined: Tools to Be Developed" section.

Functional/Structural Image Analyses Combined: Currently Available Tools and Comparison of Traditional and High-dimensional Warping Algorithms: In addition to more traditional functional image analyses (i.e., SPM99), we will use cortical surface matching algorithms developed at LONI (Thompson et al., 1997; Thompson et al., 2000b; Thompson et al., 2001a) to disambiguate brain surface abnormalities between FAS and control subjects before comparing differences in brain activation. These methods are described in the "Cortical Surface Matching for Improved Detection of Functional Activity" section of the preliminary studies.

Essentially, nonlinear elastic matching approaches have been engineered to compare and integrate functional activation data across subjects, and relate functional features to underlying anatomical deficits (Rex et al., 2001). These methods will be statistically compared to the more traditional analyses where automated linearly registered signal-based image average is applied. To accomplish this, we will conduct group comparisons (FAS vs. Control) with affine alignment (Woods et al., 1993) for rest vs activation for the various functional activation paradigms used by Consortium members and assess the volume of voxels activated at a given statistical threshold (e.g., $p < 0.001$). The difference in overall volume, cluster size, magnitude, and localization of activation will be assessed between the two strategies. In addition to the volume of activation, we will assess the cluster size and magnitude of the resulting statistical parametric maps by creating measures of the extent, total size, and magnitude of all suprathreshold voxels for each contrast, and comparing those features between the two warping algorithms. Differences in signal to noise and the reduction of the effects of confounds on parameter estimation will also be assessed by computing F-distributed statistical maps. These maps will assess the increase in model fit at each parameter location on cortex after high-dimensional warping, relative to the fit obtained after only linear alignment. Note that, for each contrast, this produces a statistical map revealing where, and to what degree, the model residuals were reduced by applying the cortical pattern matching approach. We predict that greater volumes of activation and greater significance (i.e., stronger

suprathreshold significance) will be observed with the higher dimensional warping algorithm than with the more traditional analyses.

Functional/Structural Image Analyses Combined: Tools to Be Developed: We will also develop new mathematical algorithms to empower the detection of informative linkages between structure and function in the FAS and normal cohorts. This extends extensive prior work in algorithm development for image analysis and computational anatomy, which have been widely used for analyzing pediatric and adult neuroimaging data (Narr et al., 2000; Narr et al., 2001; Sowell et al., 2001b; Thompson et al., 2001d; Thompson et al., 2001c; Thompson et al., 2001b; Narr et al., 2002; Sowell et al., 2002a; Sowell et al., 2002c; Sowell et al., 2003). For the past 7 years, we have been developing an extensive set of novel algorithms for detecting patterns of abnormal brain structure in diseased populations. These projects have generated 150+ publications in journals spanning neuroscience, engineering, mathematical and clinical fields.

We will develop computational algorithms (1) to permit correlation of structural deficits and functional activation point wise across the cortex, enabling these links to be detected and visualized statistically; and (2) to empower the statistical detection of functional and structural signals at the cortex. Both of these sets of algorithms will exploit the surface-based parametric models of the cortex, to uncover new features of anatomy and function and their linkage in FASD.

Specific Aim 4: "Correlation with Other Core Data: We will assess for relationships between the data collected and analyzed within the Imaging Core, and data collected by the other projects and cores in this Consortium such as the Dysmorphology Core, the Neurobehavioral Core, and the Facial Imaging Core. We currently have statistical tools which allow us to map linkages (via correlation, multiple regression, multivariate, non-linear regression) between brain morphology (i.e., gray matter density, local brain size) at every brain surface point and any measure collected by the various other projects and cores."

Understanding relationships between brain morphology and other behavioral and biological measures is critical to a better understanding of the effects of prenatal alcohol exposure on the brain. Any number of variables can be used in point by point statistical analyses of various features of brain morphology. We can create statistical maps showing the relationship (i.e., correlation) between, gray matter density and neurobehavioral scores on a working memory task, for example. These maps will provide localized information as to which regions of the brain are related to which cognitive functions, and if these brain-behavior relationships are altered as a function of prenatal alcohol exposure. Similar analyses can be done with data from the facial imaging core, and the dysmorpholgy core. We are continually adapting more statistical models which are integrated with our brain surface mapping software. Currently we can conduct correlation, multiple regression (non-linear tests, interactions, etc.), and t-tests on a point-by-point basis for creation of statistical brain maps. Work is underway to incorporate more sophisticated mixed model statistics for assessment of longitudinal data. Further, it will be possible to obtain discrete descriptors of brain morphology, the location of the posterior extent of the corpus callosum in each individual for example, for more detailed correlations with data from the other cores (analyses conducted by other core investigators). Shown in Figure 16 is a statistical map of facial anatomy (face surface renderings created from the MRI data and matched in the same way as brain surface anatomy, only facial anatomical landmarks are used) as it correlates with brain anatomy in the most posterior point in the corpus callosum in 11 control and 6 FAS subjects. This pilot analysis illustrates the flexibility with which we can correlate diverse data sets, and incorporate them in to 3D statistical maps. It is expected that hypothesis driven analyses will be conducted as Consortium members interact through data analysis for each core.

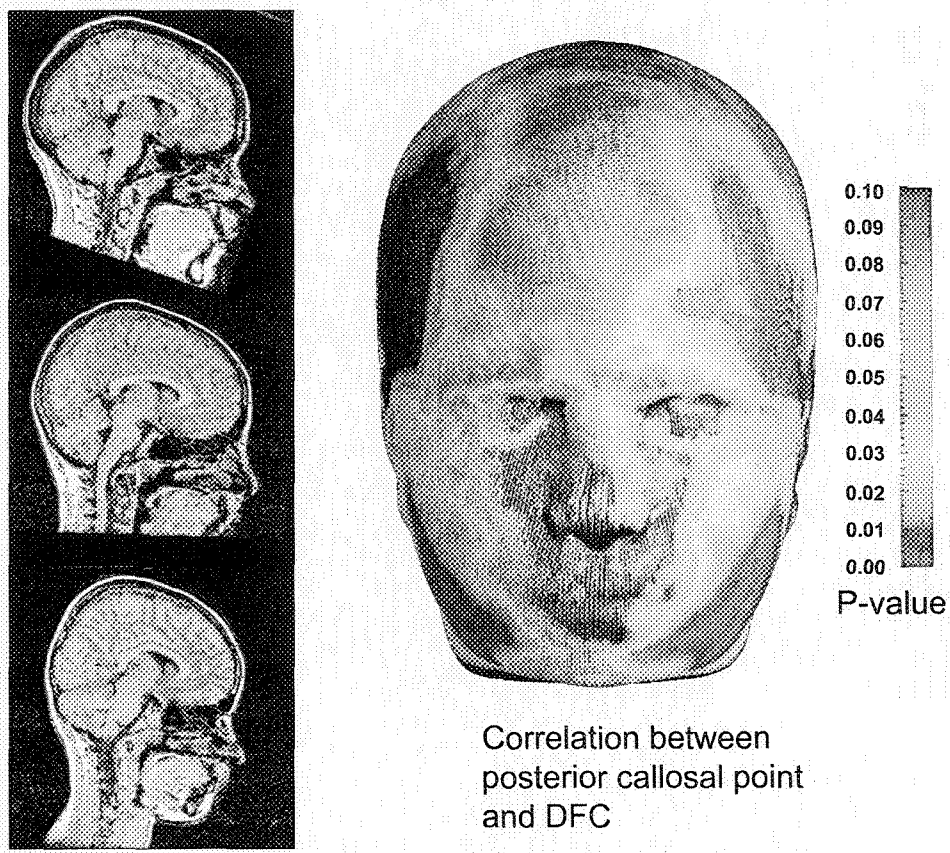

Figure 16: A statistical map of the correlation between brain anatomy measured as the y dimension (anterior/posterior) stereotaxic location of the most posterior point in the corpus callosum and facial anatomy measured on the surface renderings of each of 11 control and 6 FAS subjects studied earlier in our brain surface analyses. The most posterior point in the corpus callosum is highlighted in blue on 3 representative subjects brain MR data (left). The statistical face map (right) is color coded according to the color bar and regions where the location of the facial anatomy is correlated significantly with the location of the callosal posterior point are highlighted in warmer colors.

Time Line

	Year 1	Year 2	Year 3	Year 4	Year 5
Specific Aim 1					
Protocol Establishment					
Phantom Studies					
Specific Aim 2					
Automated Tool Adaptation and					
Distribution					
Web/email Support of Tools					
Specific Aim 3					
Adaptation of More Advanced					
Image Analysis Tools					
Analyze Consortium Data with					
Advanced Image Analysis					
Specific Aim 4					
Correlation with Other Core Data					
Miscellaneous					
Manuscript Preparation					

E. Human Subjects

Brain image and behavioral data **WILL NOT** be collected directly by the Imaging Core in this Consortium, though data collected by other Consortium members will be analyzed. Each Consortium project will provide human subjects information. However, Image and behavioral data on FASD and control subjects will be collected by the Imaging Core investigators using funding from another source (NIDA R21 DA015878-01, PI ERS), and complete IRB approval has been obtained for that project. Thus we will provide information pertaining to that project here, and similar information will be provided in the other Consortium projects who will collect imaging data.

Project NIDA R21 DA015878-01, PI ERS:

All subjects and their parents will be fully informed of the nature of the study, potential risks, and their rights as subjects under UCLA Human Subject Protection guidelines. The UCLA HSPC has given approval for performing these studies.

Protection of Human Subjects :

1.) **Risks to the Subjects:** This proposal will involve the study of 8 adult normal volunteers, 20 high functioning (IQ > 70) FAS children aged 7 to 18, and 20 age, gender and SES-matched control children as human subjects. Both male and female subjects will be studied. Subjects will be screened via parent/caretaker interview conducted by one or more of the co-investigators in this study. **Inclusion:** Children and adolescents (between 7 and 18 years of age) previously diagnosed with FAS will be recruited as will normally developing children in the same age range. **Exclusion: a)** Children with IQs less than 70 who may be unable to understand MRI procedures and provide informed consent will be excluded; **b)** Children less than 7 years of age who may be unable to tolerate MRI (i.e., unable to sit still in the scanner for periods of up to 20 minutes at a time) will be excluded; **c)** Children who have had heavy exposure to other drugs in utero will be excluded; **d)** Children who do not have a good grasp of the English language cannot be validly tested with the functional imaging paradigms utilized in this study, and thus will also be excluded. **Vulnerable Subjects:** Children will be included in this study and some of them will be intellectually impaired relative to their non-affected age-mates. All children will be able to provide informed consent/assent given that we are intentionally excluding children with IQs less than 70 (mental retardation range). Given the importance of determining the impact of prenatal alcohol exposure on child brain and cognitive development, and the lack of any dangerous or invasive procedures, the benefits of this study outweigh the risks for the inclusion of a vulnerable population. **Sources of Materials:** Data gathered are in the form of digital images, and neuropsychological evaluation results. These materials are intended to be used solely for research purposes. On rare occasions the MRI scans will reveal lesions not already known to the team. In this unlikely event, patients and their families will be given the opportunity to release their medical records to the treating clinicians. **Potential Risks:** This study involves non-invasive techniques. The clinical testing (IQ) involves paper-and-pencil tests in which the major risks are fatigue, boredom, or occasionally frustration with the tests. Risks of MRI scanning are associated with bringing unsafe metal devices into the scanner. This risk is minimized by carefully screening each subject, and checking subjects for any metal objects. In addition, the MRI scanner can be frightening for some children. We minimize this risk by exposing the child to the scanner in advance and offering training "desensitization" sessions, having "virtual reality" goggles to watch television during the scans, and by giving the subjects and "emergency escape" button which they can press if they want to leave the scanner. We offer ear protection against any risk of the noisy scan environment. In over 200 scans on children, we have not had any adverse events.

2.) Adequacy of Protection Against Risk: **Recruitment and Informed Consent:** Approximately 20 children and adolescents with prenatal exposure to alcohol will be recruited in 4 different ways. 1) Through referrals from the UCLA Departments of Pediatrics and Genetics. 2) Through referrals from Dr. Mary O'Connor in the UCLA Department of Psychiatry (an Investigator on this proposal). 3) Through referrals from physicians at the King-drew Medical Center and the UCLA Medical Center. 4) Through referrals from Dr. Edward Riley (a

consultant on this proposal). Normal control subjects will be recruited through flyers posted in the community. Parental consent will be obtained for all subjects and assent will be obtained from all children. While the alcohol-exposed subjects studied will likely have some cognitive impairment, we are excluding individuals who fall into the mentally retarded range of intellectual functioning. Thus, all subjects are likely to understand the study procedures. Subjects meeting the study criteria will be scheduled to come to UCLA for the initial evaluation. At that time, the entire experiment and the rationale for it will be explained to the subject in a face-to-face discussion with either Elizabeth Sowell, Ph.D. (Principal Investigator) or Susan Bookheimer, Ph.D. (Co-Investigator). The subject and parents will be encouraged to ask any questions about points that he/she does not understand. The informed consent form will then be given to children and their parents and they will be asked to read it carefully. Also made explicit at the time of the initial discussion will be the participation payment of $15 per hour for each subject who undergoes neuropsychological assessment and examination with MRI and fMRI. Subjects will be informed that they may withdraw from the experiment at any time without any undue pressure from the experimenters to retain participation. Then, if the child gives assent, the parent will be asked to sign the consent form. **Protection Against Risk:** Subjects will be screened via interview and questionnaire for metal in their bodies before exposure to the magnet. The desensitization session in the scanner prior to the actual MRI scan is designed to reduce potential anxiety or discomfort associated with the enclosed environment and loud scanner noise.

3.) Potential Benefits of Proposed Research to the Subjects and Others: The potential benefits from participation in the study include a detailed examination of the brain. However, this is not likely to be of great benefit to this population of children.

4.) Importance of the Knowledge to be Gained: The risks of this non-invasive technology for assessment of normal and abnormal brain development are relatively low given the benefits to humanity of a more detailed understanding of the effects of prenatal alcohol exposure on structural and functional brain development.

Inclusion of Women:

This proposal will involve the study of 7 adult normal volunteers, 20 high functioning (IQ > 70) FAS children aged 7 to 18, and 20 gender and SES-matched control children as human subjects. Both male and female subjects will be studied.

Inclusion of Minorities:

The Los Angeles community is very ethnically diverse, and our research will strive to maintain this diversity in our experiments. Our experience thus far in our studies of alcohol exposed individuals (In the Studies of Dr. Mary O'Connor) have included an ethnic make up of 62% White, not of Hispanic Origin, 20% Black, not of Hispanic Origin, 6% Hispanic, 0% Asian/Pacific Islander, and 4% other. We predict that a similar distribution will be available for recruitment for these proposed studies and we will attempt to obtain a control sample with a similar ethnic distribution to the FAS subjects.

Inclusion of Children:

Populations of interest in the proposed studies are children and adolescents.

F. Vertebrate Animals

N/A

G. Literature Cited

Abel EL, Sokol RJ (1987) Incidence of fetal alcohol syndrome and economic impact of FAS-related anomalies. Drug Alcohol Depend 19:51-70.

Archibald SL, Fennema-Notestine C, Gamst A, Riley EP, Mattson SN, Jernigan TL (2001) Brain dysmorphology in individuals with severe prenatal alcohol exposure. Dev Med Child Neurol 43:148-154.

Bandettini PA, Jesmanowicz A, Wong EC, Hyde JS (1993) Processing strategies for time-course data sets in functional MRI of the human brain. Magn Reson Med 30:161-173.

Bookstein FL, Sampson PD, Streissguth AP, Connor PD (2001) Geometric morphometrics of corpus callosum and subcortical structures in the fetal-alcohol-affected brain. Teratology 64:4-32.

Brodmann K (1909) Vergleichende Lokalisationlehre Der Grosshirnrinde in ihren' Prinzipien dargestellt auf Grund in Zellenbaues. Leipzig: J. A. Barth.

Cabeza R, Nyberg L (2000) Imaging cognition II: An empirical review of 275 PET and fMRI studies. J Cogn Neurosci 12:1-47.

Church MW, Abel EL (1998) Fetal alcohol syndrome. Hearing, speech, language, and vestibular disorders. Obstet Gynecol Clin North Am 25:85-97.

Clark CM, Li D, Conry J, Conry R, Loock C (2000) Structural and functional brain integrity of fetal alcohol syndrome in nonretarded cases. Pediatrics 105:1096-1099.

Coles CD, Platzman KA, Raskind-Hood CL, Brown RT, Falek A, Smith IE (1997) A comparison of children affected by prenatal alcohol exposure and attention deficit, hyperactivity disorder. Alcoholism, Clinical and Experimental Research 21:150-161.

Dogdas B, Shattuck DW, Leahy RM (2002) Segmentation of Skull in 3D Human MRI using Mathematical Morphology. In: Medical Imaging 2002: Image Processing (Fitzpatrick JM, ed), pp 1553-1562: Proc. SPIE.

Evans AC, Collins DL, Holmes CJ (1996) Automatic 3D Regional MRI Segmentation and Statistical Probabilistic Anatomical Maps. New York: Academic Press.

Filippi M, van Waesberghe JH, Horsfield MA, Bressi S, Gasperini C, Yousry TA, Gawne-Cain ML, Morrissey SP, Rocca MA, Barkhof F, Lycklama a Nijeholt GJ, Bastianello S, Miller DH (1997) Interscanner variation in brain MRI lesion load measurements in MS: implications for clinical trials. Neurology 49:371-377.

Friston KJ, Holmes AP, Worsley KJ, Poline J-B, Frith CD, Frackowiak RSJ (1995) Statistical parametric maps in functional imaging: A general linear approach. Human Brain Mapping 2:189-210.

Janzen LA, Nanson JL, Block GW (1995) Neuropsychological evaluation of preschoolers with fetal alcohol syndrome. Neurotoxicol Teratol 17:273-279.

Jones KL, Smith DW (1973) Recognition of the fetal alcohol syndrome in early infancy. Lancet 2:999-1001.

Konishi S, Nakajima K, Uchida I, Kikyo H, Kameyama M, Miyashita Y (1999) Common inhibitory mechanism in human inferior prefrontal cortex revealed by event-related functional MRI. Brain 122:981-991.

Lezak MD (1995) Neuropsychological Assessment, 3rd Edition. New York: Oxford University Press.

Lorensen W, Harvey W (1987) Marching cubes: A high resolution 3D surface construction algorithm. ACM Computer Graphics 21:163-169.

MacDonald D, Avis D, Evans A (1994) Multiple surface identification and matching in magnetic resonance images. Proceedings Visualization in Biomedical Computing 2359:160-169.

Mattson SN, Riley EP (1998) A review of the neurobehavioral deficits in children with fetal alcohol syndrome or prenatal exposure to alcohol. Alcoholism, Clinical and Experimental Research 22:279-294.

Mattson SN, Riley EP (1999) Implicit and explicit memory functioning in children with heavy prenatal alcohol exposure. Journal of the International Neuropsychological Society 5:462-471.

Mattson SN, Riley EP, Delis DC, Stern C, Jones KL (1996) Verbal learning and memory in children with fetal alcohol syndrome. Alcoholism, Clinical and Experimental Research 20:810-816.

Mattson SN, Riley EP, Gramling L, Delis DC, Jones KL (1998) Neuropsychological comparison of alcohol-exposed children with or without physical features of fetal alcohol syndrome. Neuropsychology 12:146-153.

Mattson SN, Goodman AM, Caine C, Delis DC, Riley EP (1999) Executive functioning in children with heavy prenatal alcohol exposure. Alcoholism, Clinical and Experimental Research 23:1808-1815.

Mazziotta JC, Toga AW, Evans A, Fox P, Lancaster J (1995) A probabilistic atlas of the human brain: theory and rationale for its development. The International Consortium for Brain Mapping (ICBM). Neuroimage 2:89-101.

Narr K, Thompson P, Sharma T, Moussai J, Zoumalan C, Rayman J, Toga A (2001) Three-dimensional mapping of gyral shape and cortical surface asymmetries in schizophrenia: gender effects. Am J Psychiatry 158:244-255.

Narr KL, Thompson PM, Sharma T, Moussai J, Cannestra AF, Toga AW (2000) Mapping morphology of the corpus callosum in schizophrenia. Cerebral Cortex 10:40-49.

Narr KL, Cannon TD, Woods RP, Thompson PM, Kim S, Asunction D, van Erp TG, Poutanen VP, Huttunen M, Lonnqvist J, Standerksjold-Nordenstam CG, Kaprio J, Mazziotta JC, Toga AW (2002) Genetic contributions to altered callosal morphology in schizophrenia. J Neurosci 22:3720-3729.

Olson HC, Feldman JJ, Streissguth AP, Sampson PD, Bookstein FL (1998) Neuropsychological deficits in adolescents with fetal alcohol syndrome: clinical findings. Alcoholism, Clinical and Experimental Research 22:1998-2012.

Patwardhan AJ, Eliez S, Warsofsky IS, Glover GH, White CD, Giedd JN, Peterson BS, Rojas DC, Reiss AL (2001) Effects of image orientation on the comparability of pediatric brain volumes using three-dimensional MR data. J Comput Assist Tomogr 25:452-457.

Peterson BS, Staib L, Scahill L, Zhang H, Anderson C, Leckman JF, Cohen DJ, Gore JC, Albert J, Webster R (2001) Regional brain and ventricular volumes in Tourette syndrome. Arch Gen Psychiatry 58:427-440.

Pitiot A, Toga AW, Thompson PM (2002) Adaptive elastic segmentation of brain MRI via shape-model-guided evolutionary programming. IEEE Trans Med Imaging 21:910-923.

Rex DE, Ma JQ, Toga AW (In Press) The LONI Pipeline Processing Environment.

Rex DE, Pouratian N, Sicotte NL, Toga AW (2001) Locational Effect of Brain Masses on fMRI of Tongue Movement (Abstract). NeuroImage 13:S232.

Riikonen R, Salonen I, Partanen K, Verho S (1999) Brain perfusion SPECT and MRI in foetal alcohol syndrome. Developmental Medicine and Child Neurology 41:652-659.

Roebuck TM, Mattson SN, Riley EP (1998) A review of the neuroanatomical findings in children with fetal alcohol syndrome or prenatal exposure to alcohol. Alcoholism, Clinical and Experimental Research 22:339-344.

Roebuck TM, Mattson SN, Riley EP (1999) Behavioral and psychosocial profiles of alcohol-exposed children. Alcoholism, Clinical and Experimental Research 23:1070-1076.

Shattuck DW, Leahy RM (2001) Automated graph-based analysis and correction of cortical volume topology. IEEE Trans Med Imaging 20:1167-1177.

Shattuck DW, Leahy RM (2002) BrainSuite: an automated cortical surface identification tool. Med Image Anal 6:129-142.

Shattuck DW, Sandor-Leahy SR, Schaper KA, Rottenberg DA, Leahy RM (2001) Magnetic resonance image tissue classification using a partial volume model. Neuroimage 13:856-876.

Sled JG, Zijdenbos AP, Evans AC (1998) A nonparametric method for automatic correction of intensity nonuniformity in MRI data. IEEE Transactions on Medical Imaging 17:87-97.

Sowell ER, Thompson PM, Tessner KD, Toga AW (2001a) Mapping continued brain growth and gray matter density reduction in dorsal frontal cortex: Inverse relationships during postadolescent brain maturation. J Neurosci 21:8819-8829.

Sowell ER, Mattson SN, Thompson PM, Jernigan TL, Riley EP, Toga AW (2001b) Mapping Callosal Morphology and Cognitive Correlates: Effects of Heavy Prenatal Alcohol Exposure. Neurology 57:235-244.

Sowell ER, Peterson BS, Thompson PM, Welcome SE, Henkenius AL, Toga AW (2003) Mapping Cortical Change Across the Human Life Span. Nature Neuroscience 6:309-315.

Sowell ER, Thompson PM, Welcome SE, Henkenius AL, Toga AW, Peterson BS (Submitted) Cortical Abnormalities in Children and Adolescents with Attention Deficit Hyperactivity Disorder.

Sowell ER, Thompson PM, Mattson SN, Tessner KD, Jernigan TL, Riley EP, Toga AW (2001c) Voxel-based morphometric analyses of the brain in children and adolescents prenatally exposed to alcohol. Neuroreport 12:515-523.

Sowell ER, Thompson PM, Mattson SN, Tessner KD, Jernigan TL, Riley EP, Toga AW (2002a) Regional brain shape abnormalities persist into adolescence after heavy prenatal alcohol exposure. Cerebral Cortex 12:856-865.

Sowell ER, Thompson PM, Rex D, Kornsand D, Tessner KD, Jernigan TL, Toga AW (2002b) Mapping sulcal pattern asymmetry and local cortical surface gray matter distribution in vivo: maturation in perisylvian cortices. Cereb Cortex 12:17-26.

Sowell ER, Thompson PM, Peterson BS, Mattson SN, Welcome SE, Henkenius AL, Riley EP, Jernigan TL, Toga AW (2002c) Mapping Cortical Gray Matter Asymmetry Patterns in Adolescents with Heavy Prenatal Alcohol Exposure. Neuro Image 17:1807-1819.

Streissguth AP, Bookstein FL, Sampson PD, Bar HM (1995) Attention: Prenatal alcohol and continuities of vigilance and attentional problems from 4 through 14 years. Development and Psychopathology 7:419-446.

Swayze VW, Johnson VP, Hanson JW, Piven J, Sato Y, Giedd JN, Mosnik D, Andreasen NC (1997) Magnetic resonance imaging of brain anomalies in fetal alcohol syndrome. Pediatrics 99:232-240.

Thompson PM, Toga AW (1997) Detection, visualization and animation of abnormal anatomic structure with a deformable probabilistic brain atlas based on random vector field transformations. Medical Image Analysis 1:271-294.

Thompson PM, Woods RP, Mega MS, Toga AW (2000a) Mathematical/computational challenges in creating deformable and probabilistic atlases of the human brain. Human Brain Mapping 9:81-92.

Thompson PM, Mega MS, Vidal C, Rapoport JL, Toga AW (2001a) Detecting Disease-Specific Patterns of Brain Structure using Cortical Pattern Matching and a Population-based Probabilistic Brain Atlas. In: IEEE Conference on InformationProcessing in Medical Imaging (IPMI) (Insana M, Leahy R, eds), pp 488-501: Springer-Verlag.

Thompson PM, MacDonald D, Mega MS, Holmes CJ, Evans AC, Toga AW (1997) Detection and mapping of abnormal brain structure with a probabilistic atlas of cortical surfaces. Journal of Computer Assisted Tomography 21:567-581.

Thompson PM, Mega MS, Narr KL, Sowell ER, Blanton RE, Toga AW (2000b) Brain Image Analysis and Atlas Construction. In: SPIE Handbook on Medical Image Analysis (Fitzpatrick M, Sonka M, eds): Society of Photo-Optical Instrumentation Engineers (SPIE) Press.

Thompson PM, Vidal C, Giedd JN, Gochman P, Blumenthal J, Nicolson R, Toga AW, Rapoport JL (2001b) Mapping adolescent brain change reveals dynamic wave of accelerated gray matter loss in very early-onset schizophrenia. Proc Natl Acad Sci U S A 98:11650-11655.

Thompson PM, Mega MS, Woods RP, Zoumalan CI, Lindshield CJ, Blanton RE, Moussai J, Holmes CJ, Cummings JL, Toga AW (2001c) Cortical Change in Alzheimer's Disease Detected with a Disease-specific Population-based Brain Atlas. Cereb Cortex 11:1-16.

Thompson PM, Cannon TD, Narr KL, van Erp T, Poutanen VP, Huttunen M, Lonnqvist J, Standertskjold-Nordenstam CG, Kaprio J, Khaledy M, Dail R, Zoumalan CI, Toga AW (2001d) Genetic influences on brain structure. Nat Neurosci 4:1253-1258.

Uecker A, Nadel L (1996) Spatial locations gone awry: object and spatial memory deficits in children with fetal alcohol syndrome. Neuropsychologia 34:209-223.

Wang L, Lai HM, Barker GJ, Miller DH, Tofts PS (1998) Correction for variations in MRI scanner sensitivity in brain studies with histogram matching. Magn Reson Med 39:322-327.

Woods RP, Mazziotta JC, Cherry SR (1993) MRI-PET registration with automated algorithm. Journal of Computer Assisted Tomography 17:536-546.

Woods RP, Grafton ST, Holmes CJ, Cherry SR, Mazziotta JC (1998a) Automated image registration: I. General methods and intrasubject, intramodality validation. J Comput Assist Tomogr 22:139-152.

Woods RP, Grafton ST, Watson JD, Sicotte NL, Mazziotta JC (1998b) Automated image registration: II. Intersubject validation of linear and nonlinear models. J Comput Assist Tomogr 22:153-165.